Emodin, as a mitochondrial uncoupler, induces strong decreases in adenosine triphosphate (ATP) levels and proliferation of B16F10 cells, owing to their poor glycolytic reserve

AUTHOR(S):

Sugiyama, Yuma; Shudo, Toshiyuki; Hosokawa, Sho; Watanabe, Aki; Nakano, Masaki; Kakizuka, Akira

CITATION:

Sugiyama, Yuma ...[et al]. Emodin, as a mitochondrial uncoupler, induces strong decreases in adenosine triphosphate (ATP) levels and proliferation of B16F10 cells, owing to their poor glycolytic reserve. Genes to Cells 2019, 24(8): 569-584

ISSUE DATE:

2019-08

URL:

http://hdl.handle.net/2433/245222

Emodin, as a mitochondrial uncoupler, induces strong decreases in adenosine triphosphate (ATP) levels and proliferation of B16F10 cells, owing to their poor glycolytic reserve

Yuma Sugiyama[1], Toshiyuki Shudo[1], Sho Hosokawa[1], Aki Watanabe[1], Masaki Nakano[1], Akira Kakizuka[1,*]

Graduate School of Biostudies, Laboratory of Functional Biology, Kyoto University, Kyoto, Japan

Correspondence Akira Kakizuka, Graduate School of Biostudies, Laboratory of Functional Biology, Kyoto University, Yoshidakonoe, Sakyo-ku, Kyoto 606-8501, Japan. Email: Kakizuka@lif.kyoto-u.ac.jp

KEYWORDS
adenosine triphosphate, emodin, glycolytic reserve, melanoma, uncoupler

Abstract

Many types of cancer cells show a characteristic increase in glycolysis, which is called the "Warburg effect." By screening plant extracts, we identified one that decreases cellular adenosine triphosphate (ATP) levels and suppresses proliferation of malignant melanoma B16F10 cells, but not of noncancerous MEF cells. We showed that its active ingredient is emodin, which showed strong antiproliferative effects on B16F10 cells both in vitro and in vivo. Moreover, we also found that emodin can function as a mitochondrial uncoupler. Consistently, three known mitochondrial uncouplers also displayed potent antiproliferative effects and preferential cellular ATP reduction in B16F10 cells, but not in MEF cells. These uncouplers provoked comparable mitochondrial uncoupling in both cell types, but they manifested dramatically different cellular effects. Namely in MEF cells, these uncouplers induced three to fivefold increases in glycolysis from the basal state, and this compensatory activation appeared to be responsible for the maintenance of cellular ATP levels. In contrast, B16F10 cells treated with the uncouplers showed less than a twofold enhancement of glycolysis, which was not sufficient to compensate for the decrease of ATP production. Together, these results raise the possibility that uncouplers could be effective therapeutic agents specifically for cancer cells with prominent "Warburg effect."

1 | INTRODUCTION

Even with the impressive advances in medical care over the last several decades, about one out of two Japanese suffers from cancer over their lifetime, and one third of Japanese die of cancer. One of the most prominent characteristics of cancer cells, regardless of type or stage, is their uncontrolled, aggressive proliferation. Such aggressive proliferation requires a vast amount of cellular energy in the form of adenosine triphosphate (ATP), as compared with noncancerous cells, as cell proliferation entails many energy-consuming steps, for example, synthesis of proteins and RNAs (rRNA, mRNA and tRNA), DNA replication and cytokinesis (Buttgereit & Brand, 1995; Gibbons & Rowe, 1965; Summers & Gibbons, 1971). As a consequence, cancer cells should be sensitive to ATP depletion by various means.

It is well known that many types of cancer cells show a characteristic increase in glycolysis, even in aerobic conditions, a phenomenon is called “Warburg effect” (Warburg, 1956; Warburg, Posener, & Negelein, 1924). Thus, glycolysis has garnered considerable interest as a possible therapeutic target. From this point of view, 2-deoxy-D-glucose (2- DG), a nonmetabolizable glucose analogue that inhibits glycolytic hexokinase, had been assessed as an anticancer drug in clinical trials. Disappointingly, however, patients treated with 2-DG showed severe side effects, so this drug is now under

evaluation in combined therapies with other chemotherapeutic compounds (Dwarakanath & Jain, 2009; Mohanti et al., 1996; Singh et al., 2005; Vander Heiden, 2011).

Recent epidemiologic studies have shown that diabetic patients treated with metformin manifest lower incidence of various types of cancers, such as breast cancer, colorectal cancer, pancreatic cancer and lung cancer (Bodmer, Meier, Krahenbuhl, Jick, & Meier, 2010; Evans, Donnelly, Emslie- Smith, Alessi, & Morris, 2005; Vernieri et al., 2016; Yin, Zhou, Gorak, & Quddus, 2013; Zhang et al., 2014). In 2000, it was reported that a target of metformin in cancer cells was mitochondrial respiratory chain complex I (El-Mir et al., 2000; Owen, Doran, & Halestrap, 2000), and this drug is now being tested in clinical trials for different types of cancers (Vernieri et al., 2016). In preclinical research, there are two types of compounds that are expected to be efficacious as new anticancer drugs, which also target the mitochondrial energy metabolism (Weinberg & Chandel, 2015). The first one, tigecycline, is an inhibitor of translation of electron transport chain (ETC) proteins, (Skrtić et al., 2011), and the second one is Gamitrinib which inhibits heat shock protein-90 (HSP90) and tumor necrosis factor receptor-associated protein- 1 (TRAP-1) ATPase. This inhibitor lead to a decrease of ATP production from oxidative phosphorylation (OXPHOS) (Chae et al., 2012).

Malignant melanoma has the dubious distinction of having one of the worst

105 prognoses, because of its aggressive metastatic nature from early stages. Melanoma is
106 responsible for over 75% of skin cancer death (Corrie, Hategan, Fife, & Parkinson, 2014),
107 and its incidence is rapidly increasing (Siegel, Miller, & Jemal, 2018). The two-year
108 overall survival rate of malignant melanoma patients at stage IV is only 10.7% (Sandru,
109 Voinea, Panaitescu, & Blidaru, 2014). Recently, some molecularly targeted therapies
110 have achieved extensive attention as new melanoma treatments, like vemurafenib
111 and nivolumab (Schadendorf et al., 2018). However, the treatments by vemurafenib, a
112 specific inhibitor of BRAF V600E, have allowed responsive tumors to be resistant to this
113 chemotherapy (Flaherty et al., 2010). On 2014, a PD-1 blocking antibody drug,
114 "nivolumab," was approved as a new drug, but the objective response rate to treatment of
115 metastatic melanoma without a BRAF mutation was not satisfying, 40% (Robert et al.,
116 2015). Thus, melanoma remains one of the most refractory neoplasms in spite of these
117 energetic studies, and it is an urgent need to develop a more effective strategy for the
118 treatment.

119 B16F10 cells, which were established from a mouse malignant melanoma (Fidler,
120 1973), serve as a model to examine the efficacies of experimental drugs in vitro and in
121 vivo. In this study, we evaluated compounds that reduce ATP levels in B16F10 cells and
122 found a plant extract from rhizomes of *Polygonum cuspidatum* (RPC). This plant extract

has long been administrated to human body as a component of a traditional medicine, and various types of pharmacological effects are known like treating cough, hepatitis, jaundice, arthralgia and skin burns. Although recent studies reported that this extract has antiviral, antimicrobial, anti-inflammatory, neuroprotective and cardioprotective activities (Peng, Qin, Li, & Zhou, 2013; Zhang, Li, Kwok, Zhang, & Chan, 2013), there are no reports about the ATP reduction in cancer cells. Here, we show an active ingredient in RPC, emodin, manifests antiproliferative effects on B16F10 cells, and acts as a "mitochondrial uncoupler" following ATP down-regulation. We thus propose mitochondrial uncoupling as a potential therapeutic strategy for cancer treatment, especially for cancers with enhanced energetic demands and reduced glycolytic reserves, like melanoma.

2 | RESULTS

2.1 | Plant extracts from rhizomes of *Polygonum cuspidatum* preferentially decreases cellular ATP levels in B16F10 cells but not MEFs

We compared growth rates and metabolic activities of two mouse cell lines, malignant melanoma B16F10 and mouse embryonic fibroblasts (MEF). Proliferation rates of B16F10 cells were much higher than those of MEF cells (Figure 1a). Assuming

that highly proliferating cancer cells display enhanced energy metabolism, we compared several metabolic indicators between the two cell lines. The extracellular acidification rate (ECAR), which indicates the strength of glycolysis, was significantly higher in B16F10 cells than in MEF cells (Figure 1b); moreover, the ECAR in B16F10 cells was also higher than in HeLa (derived from cervical cancer) and A549 cells (derived from lung cancer) (Figure S1a), consistent with the notion that B16F10 cells manifest a prominent Warburg effect. The oxygen consumption rate (OCR), which indicates the strength of mitochondrial respiration, was also much higher in B16F10 cells than in MEF, HeLa and A549 cells (Figure 1c, Figure S1b). The mitochondrial membrane potential was also much higher in B16F10 cells than in MEF cells (Figure 1d). These results imply that B16F10 cells rely on active energy metabolism through not only glycolysis but also mitochondrial respiration, which likely contribute to the aggressive proliferation of these cells. We also measured ATPase activities of whole cell lysates (Manno, Noguchi, Fukushi, Motohashi, & Kakizuka, 2010) and found that the rate of ATP hydrolysis of B16F10 cell extracts was about twice the rate in MEF cell extracts (Figure 1e). These results were consistent with the notion that B16F10 cells produce and consume cellular ATP more actively than MEF cells.

On the assumption that some plant extracts used in Chinese medicine might

reduce ATP levels in highly proliferating cells, we screened more than 1,000 plant extracts and found one (extract A) that was able to decrease cellular ATP levels in B16F10 cells, but not in MEF cells (Figure 1f). Extract A was derived from rhizomes of *Polygonum cuspidatum* (RPC).

2.2 | Emodin is the principle active ingredient in the RPC extract

In order to identify active ingredients in the RPC extract, we carried out polarity-based fractionations (Figure 2a). For this purpose, we used the second lot (#2) of the RPC extract, which was prepared in a larger amount, although its activity was lower than the first lot (#1) (Figure 2b). First, we separated the extract into two fractions, water-soluble (F1) and organic-soluble (F2), by the Bligh–Dyer method. We treated B16F10 and MEF cells with each of the two fractions at 100 μg/ml for 6 hr and measured ATP levels of the cells. The results showed that the F2 fraction drastically decreased cellular ATP levels in B16F10 cells, and this effect was clearly much weaker in MEF cells (Figure 2b). Next, F2 was dissolved in 100% CHCl3, followed by solid phase extraction (SPE), and we separated it into three fractions, F2-1 (eluted by 100% CHCl3), F2-2 (eluted by CHCl3:MeOH = 4:1) and F2-3 (eluted by CHCl3:MeOH = 1:1). We then treated cells with each fraction (F2, F2-1, F2-2 or F2-3), at 30 μg/ml each for 6 hr and measured

177 cellular ATP levels. Two fractions, F2 and F2-1, showed significant reductions of
178 cellular ATP levels in B16F10 cells, and the effect was much more pronounced with the
179 F2-1 treatment than the F2 treatment (Figure 2c).

180 HPLC analysis showed only two prominent peaks in F2-1, and these peaks were
181 much smaller in F2-2 and F2-3 (Figure 2d and Figure S2a,b). We noticed from the
182 literature that these two peaks with very low polarity characteristics were most likely to
183 be emodin and physcion, abundant anthraquinones in RPC, which also have very low
184 polarity characteristics (Chu, Sun, & Liu, 2005). We then compared F2-1 with
185 commercially obtained emodin and physcion by HPLC. The retention times of the two
186 peaks in F2-1 (Peak A: 11.52 min, Peak B: 18.97 min) were very close to that of emodin
187 (11.53 min) and physcion (19.04 min), respectively (Figure 2d). Furthermore, optical
188 spectra of each peak (A or B) in F2-1 were almost identical with that of emodin or
189 physcion, respectively (Figure 2e). To confirm the structure of peak A and B, we analyzed
190 F2-1, emodin and physcion, by 1H-NMR. The chemical shifts of each peak (A or B) were
191 accurately matched with that of emodin or physcion, respectively, and molar ratio of A
192 and B was approximately 1:0.28 (Figure 2f,g) (Danielsen, Aksnes, & Francis, 1992). To
193 confirm this ratio, we compared peak areas between F2-1 and a mixed sample of emodin
194 and physcion, which was prepared at 1:0.28 molar ratio. The result showed that the area

ratio of the two peaks in F2-1 and the mixed sample were very close (Figure S3). From these results, we concluded that F2-1 was composed of two anthraquinones, emodin and physcion (Figure 2h), at a molar ratio of approximately 1:0.28.

We then treated two cell lines with 8 μg/ml of emodin or 8 μg/ml of emodin + 2.24 μg/ml of physcion (emodin: physion = 1:0.28 in molar ratio), examined the ATP levels of the cells, and found that both had similar capacities to decrease cellular ATP levels in B16F10 cells (Figure 2i). Physcion did not affect emodin's action in B16F10 cells. However, the mixure of emodin and physcion appeared to reduce ATP levels in MEF cells, although this effect was not significant. This tendency was also observed in MEF cells treated with 30 μg/ml of F2-1 (Figure 2c). From these results, we concluded that an effective ingredient in the RPC extract, which reduces ATP levels preferentially in B16F10 cells, is emodin.

2.3 | Emodin suppresses cell proliferation of B16F10 cells in vitro and in vivo

We next examined the suppressive effects of emodin on B16F10 cell proliferation. As expected, 4, 8 and 16 μg/ml of emodin showed significant suppression of proliferation of B16F10 cells (Figure 3a). In contrast, only 16 μg/ml of emodin showed significant suppression on the proliferation of MEF cells. Similar suppressive effects on

the cellular ATP levels were observed (Figure 3b, Figure S4). In these experiments, we used cisplatin as a control, which is well known to manifest severe side effects in patients, and found that cisplatin showed similar antiproliferative effects in both B16F10 and MEF cells (Figure S5a). Because its mode of action is DNA interstrand crosslinking rather than perturbation of energy homeostasis per se, cisplatin did not reduce ATP levels in both B16F10 and MEF cells (Figure S5b). Following up on emodin's ability to preferentially decrease cellular ATP levels, much more in B16F10 cells than in MEF cells, we evaluated phosphorylation (Thr172) of AMP-activated protein kinase (AMPK). Western blot analyses showed a clear increase in phosphorylation of AMPK at 8 and 16 μg/ml of emodin in B16F10 cells, compared with MEF cells (Figure 3c).

We next examined the antiproliferative effects of emodin up to 3 days in B16F10 and MEF cells (Figure 3d). 4 and 8 μg/ml emodin produced significant effects in B16F10 cells ($p < 0.005$ and $p < 0.005$, respectively), and marginal or less significant effects in MEF cells ($p = 0.571$ and $p = 0.059$, respectively). It is noteworthy that cisplatin suppressed proliferation much more effectively in MEF cells than B16F10 cells. In order to evaluate emodin's antiproliferative effects on B16F10 cells in vivo, we treated mice bearing B16F10 cell-derived tumors with emodin (50 mg kg−1 day−1), as outlined in Figure 3e. An emodin- treated group ($n = 9$) showed significant

suppressions of tumor growth at 8, 10 and 12 days after the injection of B16F10 cells, as compared to a vehicle-treated group (n = 9) (Figure 3f).

2.4 | Emodin functions as a mitochondrial uncoupler

Because emodin decreased cellular ATP levels in B16F10 cells, we next evaluated mitochondrial functions after emodin treatment. We first evaluated the mitochondrial membrane potential (MMP) by using tetramethylrhodamine methyl ester (TMRM) and we found that the addition of emodin rapidly reduced the MMP, which dropped to levels approximately 30% of those before its addition, within only 30 min (Figure 4a) (Qu et al., 2013). This effect continued up to 24 hr after its addition (Figure 4b). Notably, similar phenotypes were also observed in MEF cells. We considered two possibilities for the decrease of the MMP: inhibition of OXPHOS or proton leakage from the inner membrane space to the matrix, which would tend to decrease or enhance the oxygen consumption rate (OCR), respectively. Thus, we monitored the OCR before and following the addition of emodin; we also used carbonyl cyanide 3-chlorophenylhydrazone (CCCP), a mitochondrial uncoupler, or rotenone, a respiration inhibitor, as controls. Treatment with emodin or CCCP similarly stimulated the OCR in both cell lines, and the stimulated OCR was completely abrogated by the inhibition of the

mitochondrial respiratory chain with rotenone and antimycin (Figure 4c). It is known that cells increase OXPHOS when faced with proton leakage in order to compensate for the lack of the proton gradient between the inner membrane space and the matrix. This notion and our results support the idea that proton leakage, but not inhibition of OXPHOS, is the underlying mechanism. ATP synthetase is a well-known proton leaker. However, the enhancement of the OCR by emodin or CCCP was also induced in the presence of oligomcin, an inhibitor of ATP synthetase, indicating that ATP synthetase is not involved in this increased respiration (Figure 4d, Figure S6). It is also known that proton leakage can also be chemically induced by an uncoupler, such as CCCP. Indeed, emodin and CCCP acted very similarly to decrease the MMP and increase the OCR. CCCP combines protons in a proton-rich environment and is able to pass through the cellular membrane and then provoke the release of protons in a neutral environment. For both of these to occur, the uncoupler requires two basic features, lipophilicity and weak acidity. It is notable that two parameters, pKa and logP, are very similar between emodin and CCCP (Figure 4e) (Scifinder, 2017).

We next examined the relationship between mitochondrial uncoupling and cellular phenotypes induced by emodin. We treated both B16F10 and MEF cells with three different mitochondrial uncouplers and evaluated their effects. Treatment with

CCCP, carbonyl cyanide 4-(trifluoromethoxy)phenylhydazone (FCCP) and 2,4-dinitrophenol (DNP) all decreased MMP similarly to what we observed with the emodin treatment (Figure 4f, Figure S7). FCCP and DNP marginally and emodin and CCCP significantly reduced ATP levels (Figure 4g), and emodin and all three uncouplers preferentially showed antiproliferative effects on B16F10 cells, opposed to MEF cells (Figure 4h). Furthermore, inhibition of mitochondrial respiratory chain complex I with rotenone or metformin did not show preferential ATP reduction and antiproliferation effects in B16F10 cells rather than MEF cells (Figure 4i,j). It is notable that both inhibitors reduced the ATP levels more potently in MEF cells than in B16F10 cells (Figure 4i). From these lines of evidence, we concluded that emodin functions as a mitochondrial uncoupler (Attene-Ramos et al., 2013; Betina & Kuzela, 1987; Ubbink-Kok, Anderson, & Konings, 1986).

2.5 | Glycolytic reserve of B16F10 cells is poor compared with MEF cells

Given the enhanced sensitivity of B16F10 cells to emodin, we next focused on another energy-producing system, glycolysis, in cells treated with uncouplers. First, we measured glucose consumption in media and found that emodin and three mitochondrial uncouplers drastically enhanced glucose consumption in MEF cells, whereas only a weak

285 increase was observed with B16F10 cells (Figure 5a). Next, we monitored the
286 extracellular acidification rate (ECAR) followed by the addition of mitochondrial
287 uncouplers and 2-deoxy-D-glucose (2-DG). Because of the autofluorescence of emodin,
288 we could not obtain reliable ECAR data for cells treated with emodin in this system.
289 Nevertheless, CCCP, FCCP and DNP dramatically increased the ECAR of MEF cells, up
290 to three to five times higher than the baseline points before their addition, indicating an
291 obvious increase in glycolysis because of uncoupling (Figure 5b,c right). This
292 compensatory activation of glycolysis in the face of mitochondrial dysfunctions, termed
293 the "glycolytic reserve," could potentially maintain cellular ATP levels. By contrast, with
294 B16F10 cells, the enhancements of ECAR were only 50%–80% compared with baseline
295 levels (Figure 5b,c, left). It is notable that HeLa and A549 cells appeared to have more
296 glycolytic reserve than B16F10 cells (Figure S8a). Consistently, emodin and all three
297 uncouplers produced smaller effects on HeLa and A549 cells than on B16F10 cells
298 (Figure S8b).

299 Next, we treated B16F10 and MEF cells with emodin in various concentrations of
300 glucose and measured ATP levels by a luciferase-based assay. The result showed that, in
301 all concentrations of glucose (200, 100, 50 and 0 mg/dl), cellular ATP levels of B16F10
302 cells treated with 8 μg/ml of emodin for 6 hr clearly decreased (Figure 5d, left). In contrast,

MEF cells could not keep their ATP levels only under the glucosefree conditions (in correct, this medium included FBS-contained glucose) by treatment of 8 μg/ml of emodin for 6 hr (Figure 5d, right). And this reduction of ATP levels could not be rescued by treatment of pyruvate, a metabolite for TCA cycle (Figure S9a). Furthermore, treatment with 8 μg/ ml emodin suppressed the proliferation of MEF cells under glucose-free condition (Figure S9b,c). These results suggest that the resistance of MEF cells to emodin depends on the glycolytic reserve.

3 | DISCUSSION

Cancer cells use higher amounts of energy for their enhanced proliferation, as compared with nonmalignant normal cells, indicating the presence of cancer-specific energy metabolisms, for example, enhanced glycolysis or Warburg effects. The corresponding cancer-specific energy metabolisms have long been considered as potential targets for cancer therapy. In this regard, the down-regulation of ATP production might be a simple and effective strategy for limiting the proliferation of cancer cells. Indeed, “metformin,” which functions as an inhibitor of mitochondrial respiratory chain complex I, has been evaluated in clinical trials for cancer therapy.

We have collected more than 1,000 plant extracts and used them as sources of

chemicals with potential benefits for human health; we have previously identified "Garcinielliptone HC" from hop flower extracts as a potential prophylactic for Alzheimer's Disease (Sasaoka et al., 2014). We then hypothesized that some plant extracts might contain chemicals that can reduce ATP levels in a cancer cell-specific manner. We then screened the extracts and found that one extract, which was derived from rhizomes of *Polygonum cuspidatum* (RPC), had such activities; the extract decreased cellular ATP levels in rapidly proliferating melanoma B16F10 cells but not normal mouse embryonic fibroblast (MEF) cells. Using several analytical techniques, we identified the principle active ingredient as "emodin," an anthraquinone. "Emodin" has been repeatedly purified from many different plant extracts and been reported to elicit many cellular effects, for example, anticancer, hepatoprotective, anti-inflammatory, antimicrobial and antioxidant activities (Dong et al., 2016). These observations surprised us, because only one plant extract, RPC, effectively lowered ATP levels in B16F10 cells. These results indicate that RPC extract contains much more emodin than any other plant extracts tested.

Emodin as well as RPC extract showed very promising characteristics as potential agents for cancer therapy. Both dramatically reduced ATP levels in B16F10 cells but not in MEF cells. Concomitantly, both inhibited proliferation of B16F10 cells more potently

than MEF cells. These differential inhibitory effects present a sharp contrast to cisplatin, an anticancer drug widely used in current clinical treatments. Cisplatin did not reduce ATP levels in both B16F10 cells and MEF cells; moreover, it inhibited proliferation of both cells. It is notable that the antiproliferative effects of cisplatin were even greater on MEF cells than on B16F10 cells, which may explain some of the severe side effects of cisplatin (Tsang, Al-Fayea, & Au, 2009). With this in mind, emodin and RPC extract might produce milder side effects than cisplatin. The antiproliferative effects of emodin were also confirmed in an in vivo assay, using a mouse melanoma model in which B16F10 cells were subcutaneously implanted. Administrations of emodin (50 mg kg−1 day−1) to the mice significantly suppressed the tumor growth of B16F10 cells. These results support the idea that ATP down-regulation in cancer cells is a potential therapeutic strategy to suppress cancer cell proliferation.

What is molecular basis of the antiproliferative effect of emodin? Emodin has been shown to produce oxidative stress in cells (Qu et al., 2013; Su, Chang, Shyue, & Hsu, 2005). We thus examined the effect of N-acetyl-L-cysteine (NAC), a well-known antioxidant, on the antiproliferative effects of emodin. Treatment of 1 mM NAC, which clearly suppressed the cytotoxicity induced by H2O2, did not diminish the antiproliferative effects of emodin at all (Figure S10). We further observed that emodin

357 treatment led to stimulation of the OCR, which is usually accompanied by an elevation
358 of the MMP. However, emodin reduced the MMP. These results indicate that emodin
359 functions as a mitochondrial uncoupler. Consistently, other mitochondrial uncouplers,
360 CCCP, FCCP and DNP, also showed similar effects on the OCR and MMP. These
361 uncouplers also reduced cellular ATP levels and showed antiproliferative activities, and
362 both were prominent on B16F10 cells, but not on MEF cells. Furthermore, the chemical
363 profiles of emodin fit well with those of the uncouplers or the ionophore. Taken together,
364 we conclude that the antiproliferative effects of emodin are due to function as a
365 mitochondrial uncoupler. Some of the studies reported that emodin provokes an
366 antiproliferative activity or cell death in cancer cell lines and also mentioned various
367 molecule behaviors in cancer cells treated with emodin. For example, an activation of
368 mitochondrial apoptotic pathway, stimulated FAS ligand pathway, decreased gene
369 expression of C-MYC, lowered signals related to the cell stemness or reduced
370 protein level of ERα (Dong et al., 2016). Nevertheless, in the cancer cells treated with
371 emodin, the initial event at molecular level had been unclear. Furthermore, no studies
372 focused on emodin's noteworthy actions which we observed in this study, mitochondrial
373 uncoupling and ATP down-regulation, as a potential target to overcome cancer
374 malignancy.

375 The ability of uncouplers to lower ATP levels directed our attention to the
376 preferentially suppression of growth of cancer cells such as B16F10, as compared with
377 MEF cells. Emodin and other uncouplers were able to enhance glucose consumptions in
378 both B16F10 cells and MEF cells, but the effects were much stronger in MEF cells (300%
379 to 450% enhancements) than in B16F10 cells (170% to 190%
380 enhancements). Consistently, CCCP, FCCP and DNP were able to enhance ECAR much
381 more strongly in MEF cells than in B16F10 cells (Recall that we were unable to conduct
382 the ECAR assay with emodin because of its autofluorescence). Furthermore, MEF cells
383 could not sustain their ATP levels after the emodin stimulation under the very low
384 concentrations of glucose. These results indicated that B16F10 cells have much
385 less “glycolytic reserve” than MEF cells and thus B16F10 cells were much more sensitive
386 to emodin or other uncouplers than MEF cells, resulting in a more pronounced reduction
387 in ATP levels and suppression of the growth of B16F10 cells than MEF cells. From these
388 results, we concluded that the “glycolytic reserve” is a major determinant in maintaining
389 cellular ATP levels in response to mitochondrial uncouplers. It is notable that many
390 tumors grow in hypoxic conditions, indicating that such hypoxic cancer cells maximally
391 use glycolysis and thereby maintain less glycolytic reserve, which would further enhance
392 the Warburg effect. We thus propose ATP down-regulation by mitochondrial uncoupling

as a challenging strategy for the cancer therapy, alone or in combination with other cancer therapeutics already in use.

4 | EXPERIMENTAL PROCEDURES

4.1 | Cell culture

Both cell lines, B16F10 (obtained from Riken Bioresource Center Cell Bank) and MEF (naturally immortalized mouse embryonic fibroblasts, kindly provided by Professor Shin Yonehara (Kyoto University)), were cultured in Roswell Park Memorial Institute medium 1640 (RPMI 1640, NACALAI TESQUE). HeLa (also kindly provided by Professor Shin Yonehara (Kyoto University)) and A549 (obtained from Riken Bioresource Center Cell Bank) cell lines were maintained in Dulbecco Modified Eagle medium (DMEM-high glucose, NACALAI TESQUE). Cell culture was carried out with 10% fetal bovine serum (Sigma) in a humidified incubator with 5% carbon dioxide (CO2) at 37°C. All cells were routinely tested for Mycoplasma using MycoAlert (Lonza).

4.2 | Plant extracts and reagents

Crude plant extracts were purchased from an importer of Chinese Medicine. Reagents were as follows: emodin (Tokyo Chemical Industry), physcion (LKT Laboratories), dimethyl sulfoxide (DMSO) (NACALAI TESQUE), polyethylene glycol 400 (PEG400) (HAMPTON), cisplatin (CDDP) (Nihon Kayaku), rotenone (Sigma), antimycin (Sigma), oligomycin (Sigma), carbonyl cyanide 3-

chlorophenylhydrazone (CCCP) (NACALAI TESQUE), carbonyl cyanide 4-(trifluoromethoxy) phenylhydazone (FCCP) (Santa Cruz Biotechnology), 2,4-dinitrophenol (DNP) (Sigma), metformin (Sigma) and 2- deoxy-D-glucose (2-DG) (NACALAI TESQUE).

4.3 | Extracellular flux analysis

Extracellular acidification rate (ECAR) and the oxygen consumption rate (OCR) were measured by Seahorse Extracellular Flux Analyzer 96 (Seahorse XF96 Analyzer, Agilent) according to the manufacture's protocol. Briefly, cells were plated at 1x104 cells per well in a Seahorse XF96 Cell Culture Microplate and were cultured for approximately 24 hr. Then, media were changed to media with lower pH buffering capacity (Agilent 103676-100) followed by placing the plate in Seahorse XF96 Analyzer. Emodin or other reagents were injected at defined time points automatically. After the measurements, cells were fixed (20% formaldehyde, 2% glutaraldehyde, PBS (without Ca2+ and Mg2+) and stained with Hoechst 33342 (Invitrogen). Cell numbers were counted by counting the number of nuclei using an ArrayScan VTI High Content Platform (Thermo Fisher Scientific); then, ECAR and OCR were normalized by the cell number in each well.

447

448 **4.4 | ATPase activity assay**

449 Cells cultured in 100-mm dishes were washed with ice-cold PBS and then
450 harvested in 500 µl of ice-cold ATPase buffer (50 mM Tris-HCl, 250 mM sucrose, 5 mM
451 MgCl2, 0.5 mM EDTA, 0.3 mM DTT) using a scraper. Cells were lysed by repeated
452 passage through a 27 G needle attached to a 1cc syringe on ice, followed by centrifugation
453 at 13,000 *g*, 4°C for 10 min. The supernatants were transferred to new tubes, and aliquots
454 were subjected to a bicinchoninic acid assay (BCA, NACALAI TESQUE) to quantify
455 protein concentrations. The cell lysates were diluted with ATPase buffer to 1 µg of total
456 protein in 20 µl and incubated at 37°C for 15 min. After the incubations, 100 µM [γ-32P]
457 ATP (18.5 GBq/mmol) in 20 µl of ATPase assay buffer (1 mM HEPES[pH 7.4], 2.5
458 mM KCl, 5 mM MgCl2, 50 µM ATP, 15 mM DTT) was added to monitor ATP hydrolysis
459 reactions for 20 min. Then, 200 µl of ice-cold 8% TCA was added to quench the reactions,
460 followed by the additions of 50 µl of solution A (3.75% ammonium molybdate, 0.02 M
461 silicotungstic acid in 3 N H2SO4) and 300 µl of *n*-butyl acetate to the reactions. The
462 samples were thoroughly mixed and centrifuged at 15,000 *g* for 5 min at room
463 temperature. After the phase separation, 200 µl aliquots of the upper layer were mixed
464 with 2 ml of clear-sol II, and radioactivity, corresponding to 32P release, was

quantitated with a liquid scintillation counter (PerkinElmer). The relative radioactivities were shown as results.

4.5 | Evaluations of mitochondrial membrane potential

Cells plated on a collagen-coated glass-bottom 35-mm dish (Mat-Tek) were treated with 50 nM of tetramethylrhodamine methyl ester (TMRM) (Invitrogen) in phenol red-free RPMI 1640 (NACALAI TESQUE) with 10% FBS for 30 min at 37℃. Imaging was carried out with a Nikon Ti-E inverted microscope using a 60× objective (Nikon; CFI Plan Apo λ 60× oil: NA 1.40) which was controlled with NIS-Elements (Nikon). The following filter sets (Semrock) were used: for imaging of TMRM, 562/40 excitation filter—dichroic mirror FF593—641/75 emission filter; and for imaging of Hoechst 33342, 405/10 excitation filter—dichroic mirror FF495-520/35 emission filter. Fluorescence emissions from samples were captured with a Zyla4.2 sCMOS camera (ANDOR). Throughout the imaging, cells were maintained at 37℃ with a continuous supply of a mixture of 95% air and 5% CO_2 using a stage-top incubator (Tokai Hit). The imaging results were quantified by MetaMorph (Molecular Devices).

4.6 | Luciferase-based ATP quantification

Cells were plated in a 24-well plate and were cultured for approximately 24 hr before drug treatment. At each period (6 or 24 hr), culture media were removed and cells were gently washed with PBS. 200 µl of Glo Lysis Buffer (1×, Promega) was added to each well, and cells were incubated for 5 min. Then, the plate was agitated with a plate-shaker for 1 min and the supernatants were transferred to 96-well plate. Bioluminescence of each well was measured by an ARVO multilabel counter (PerkinElmer) using ATP assay reagent for cells (ToyoB-net). Each value of bioluminescence was normalized by the protein content, respectively, using a Protein Assay Bicinchoninate Kit (NACALAI TESQUE).

4.7 | Bligh–Dyer method

Seventy to eighty milligram of crude extract was suspended in 3.8 ml of solvent 1 (chloroform: methanol: water, 1 ml: 2 ml: 0.8 ml) by vortexing. After an incubation for 10 min at room temperature, 2 ml of solvent 2 (chloroform: water, 1 ml: 1 ml) was added and mixed by vortexing, and then incubated for 15 min at room temperature. The mixture was centrifuged at 9,100 *g* for 15 min at 4°C. The upper layer (water-soluble fraction: F1) and the lower layer (lipid-soluble fraction: F2) were separated and dried. The dried fractions were weighed. Of the crude extract, approximately 70% and 10% in F1 and F2

by weight, respectively, were recovered, whereas the remaining 20% was left in an insoluble-intermediate layer.

4.8 | Solid phase extraction

The dried lipid-soluble fraction (F2) from the Bligh–Dyer method was dissolved in chloroform, and further separation was carried out by a Sep-Pak Plus Silica column (Waters). Before loading, dissolved F2 was filtered through an Acrodisc LC 25-mm Syringe Filter with 0.45 μm PVDF Membrane (Pall corporation). The filtered F2 was loaded into the column and was eluted with 100% chloroform (F2-1), followed by chloroform: methanol (4:1) (F2-2) and chloroform: methanol (1:1) (F2-3). Each fraction was dried and dissolved in dimethyl sulfoxide (DMSO) and then subjected to the biological assay.

4.9 | HPLC analysis

Reverse-phase HPLC separations were carried out with an Alliance 2690 HT (Waters), 996 Photodiode Array Detector (Waters) and Mightysil RP-18 150–4.6 (particle size 5 μm) HPLC column (Kanto Chemical). 50 μl of filtered samples was applied to the column, which was eluted with a gradient from 0.1% TFA in acetonitrile:

519 0.1% TFA in water (40:60) to (90:10) for 30 min. The flow rate was 1.0 ml/min, and
520 the column temperature was maintained at 40°C.
521
522 **4.10 | ^{1}H-NMR**
523 ^{1}H-NMR spectra were recorded on a JNM-AL 400 (JEOL) at 400 MHz.
524 Chemical shifts were reported relative to Me4Si (δ 0.00) in DMSO-d6. Multiplicity was
525 indicated by one or more of the following: s (singlet); brs (broad singlet); and
526 d (doublet).
527
528 **4.11 | Trypan blue dye-exclusion test**
529 After the drug treatment, both floating and attaching cells were harvested into a
530 tube. The total cell suspensions from each well were centrifuged at 3,420 *g* for 5 min;
531 then, the pellets were resuspended in an aliquot of PBS. 10 μl of each respective cell
532 suspension was mixed with 10 μl of trypan blue solution (0.4%, Gibco by Life
533 Technologies), followed by cell counting using a TC10 Automated Cell Counter (Bio-
534 Rad).
535
536 **4.12 | Western blotting**

Cells were harvested in RIPA buffer (5 mM EDTA (Dojindo), 0.1% CHAPS (Dojindo), 1 mM NaF (NACALAI TESQUE), 1 mM NaVO4 (NACALAI TESQUE), 1 mM NaPPi (Dojindo), 0.5 mM PMSF (NACALAI TESQUE), 1× protease inhibitor cocktail (NACALAI TESQUE), 0.5 mM DTT (NACALAI TESQUE), 5 mM β-glycerophosphate (Sigma)), and were sonicated on ice followed by centrifugation at 4℃ at 20,400 *g* for 5 min. The supernatant was used for protein concentration determination by the BCA assay (NACALAI TESQUE). Ten μg of protein was loaded per well, was separated by 10% SDS-PAGE and was transferred to polyvinylidene fluoride membranes (Millipore). Primary antibodies were the following: anti-phospho-AMPKα (Thr172) (1:1,000, Cell Signaling Technology, #2535S), anti-AMPKα (1:1,000, Cell Signaling Techonology, #2603S), anti-actin (1:1,000, Millipore, MAB1501), anti-p53 (FL-393) (1:200, Santa Cruz Biotechnology, sc-6243) and anti-p21 (C-19) (1:200, Santa Cruz Biotechnology, sc-397). Secondary antibodies labeled with HRP were purchased from GE Healthcare, and signals were visualized by enhanced chemiluminescence (GE Healthcare).

4.13 | Tumor growth assay

B16F10 cells cultured in 100-mm dishes were treated with 0.25% trypsin and

555 harvested in culture medium (RPMI1640 supplemented with 10% FBS); then, the cells
556 were centrifuged at 160 *g* for 3 min, and the pellet was resuspended in PBS to wash out
557 the culture medium by centrifugation. After the washing, the pellet was suspended in a
558 small amount of PBS followed by cell counting, and the cell concentration was adjusted
559 to 4 × 106 cells/ml by dilution in PBS. B16F10 cells were transplanted into the right flank
560 of C57BL/6N mice (female, 7–8 weeks old) subcutaneously (2 × 105 cells/ mouse, Day
561 0). Starting on the following day (Day 1), emodin dissolved in a mixture of DMSO and
562 PEG400 (1:1) was administrated intraperitonealy at 50 mg/kg of body weight per day for
563 12 days. On Days 8, 9 and 10, tumor sizes, length (A mm), width (B mm) and height (C
564 mm) were measured, and the tumor volume was calculated by A × B×C × 0.52. All
565 animal studies were approved by the Animal Care and Use Committee of Kyoto
566 University.
567
568 **4.14 | Glucose consumption**
569 Cells were plated in a 24-well plate and were cultured for approximately 24 hr,
570 followed by treatments with 200 µl of drug-containing medium for 4 hr. The cultured
571 media supernatants were harvested and centrifuged at 3,420 *g* for 5 min.
572 Glucose concentrations in the supernatants were determined by a Glucose CII Assay Kit

(Wako) according to the manufacturer's instructions. Possible direct effects of each compound on the Glucose CII reactions were evaluated by using compound-containing media without cells, in parallel mock wells of the 24-well plate.

4.15 | Statistical analysis

The statistical significance was evaluated using Student's *t* test or Dunnett's test, where appropriate.

ACKNOWLEDGMENTS

We thank Professor James A. Hejna (Kyoto University) for critical reading of the manuscript, Professor Shin Yonehara (Kyoto University) for the gift of the MEF and HeLa cells, and members of Kakizuka Lab for discussion.

REFERENCES

Attene-Ramos, M. S., Huang, R., Sakamuru, S., Witt, K. L., Beeson, G.C., Shou, L., … Xia, M. (2013). Systematic study of mitochondrial toxicity of environmental chemicals using quantitative high throughput screening. *Chemical Research in Toxicology*, *26*(9), 1323–1332. https ://doi.org/10.1021/tx400 1754

Betina, V., & Kuzela, S. (1987). Uncoupling effect of fungal hydroxyanthraquinones on mitochondrial oxidative phosphorylation.*Chemico-Biological Interactions*, *62*(2), 179–189. https ://doi.org/10.1016/0009-2797(87)90089-5

Bodmer, M., Meier, C., Krahenbuhl, S., Jick, S. S., & Meier, C. R.(2010). Long-term metformin use is associated with decreased risk of breast cancer. *Diabetes Care*, *33*(6), 1304–1308. https ://doi.org/10.2337/dc09-1791

Buttgereit, F., & Brand, M. D. (1995). A hierarchy of ATP-consuming processes in mammalian cells. *The Biochemical Journal*, *312*(Pt 1),163–167. https ://doi.org/10.1042/bj312 0163

Chae, Y. C., Caino, M. C., Lisanti, S., Ghosh, J. C., Dohi, T., Danial, N.N., … Altieri, D. C. (2012). Control of tumor bioenergetics and survival stress signaling by mitochondrial HSP90s. *Cancer Cell*, *22*(3),331–344. https ://doi.org/10.1016/j.ccr.2012.07.015

Chu, X., Sun, A., & Liu, R. (2005). Preparative isolation and purification of five compounds from the Chinese medicinal herb *Polygonum cuspidatum* Sieb. et Zucc by high-speed counter-current chromatography.*Journal of Chromatography A*, *1097*(1–2), 33–39. https ://doi.org/10.1016/j.chroma.2005.08.008

Emslie-Smith, A. M., Alessi, D. R., & Morris, A. D. (2005). Metformin and reduced risk of cancer in diabetic patients. *BMJ*, *330*(7503), 1304–1305. https ://doi.org/10.1136/bmj.38415.708634.F7

Fidler, I. J. (1973). Selection of successive tumour lines for metastasis. *Nature New Biology*, *242*(118), 148–149. https ://doi.org/10.1038/newbi o2421 48a0

Flaherty, K. T., Puzanov, I., Kim, K. B., Ribas, A., McArthur, G. A.,Sosman, J. A., … Chapman, P. B. (2010). Inhibition of mutated, activated BRAF in metastatic melanoma. *New England Journal of Medicine*, *363*(9), 809–819. https ://doi.org/10.1056/NEJMoa1002011

Gibbons, I. R., & Rowe, A. J. (1965). Dynein: A protein with adenosine triphosphatase activity from Cilia. *Science*, *149*(3682), 424–426. https ://doi.org/10.1126/science.149.3682.424

Manno, A., Noguchi, M., Fukushi, J., Motohashi, Y., & Kakizuka, A. (2010). Enhanced ATPase activities as a primary defect of mutant valosin-containing proteins that cause inclusion body myopathy associated with Paget disease of bone and frontotemporal dementia. *Genes to Cells*, *15*(8), 911–922. https ://doi.org/10.1111/j.1365-2443.2010.01428.x

Mohanti, B. K., Rath, G. K., Anantha, N., Kannan, V., Das, B. S., Chandramouli, B. A. R., … Jain, V. (1996). Improving cancer radiotherapy with 2-deoxy-D-glucose: Phase I/II clinical trials on human cerebral gliomas. *International Journal of Radiation Oncology Biology Physics*, *35*(1), 103–111. https ://doi.org/10.1016/S0360-3016(96)85017-6

Owen, M. R., Doran, E., & Halestrap, A. P. (2000). Evidence that metformin exerts its anti-diabetic effects through inhibition of complex1 of the mitochondrial respiratory chain. *The Biochemical Journal*, *348*(Pt 3), 607–614.

Peng, W., Qin, R., Li, X., & Zhou, H. (2013). Botany, phytochemistry, pharmacology, and potential application of *Polygonum cuspidatum* Sieb.et Zucc: A review. *Journal of Ethnopharmacology*, *148*(3), 729–745. https ://doi.org/10.1016/j.jep.2013.05.007

Qu, K., Shen, N.-Y., Xu, X.-S., Su, H.-B., Wei, J.-C., Tai, M.-H., … Liu, C. (2013). Emodin induces human T cell apoptosis in vitro by ROS-mediated endoplasmic reticulum stress and mitochondrial dysfunction. *Acta Pharmacologica Sinica*, *34*(9), 1217–1228. https ://doi.org/10.1038/aps.2013.58

669
670 Robert, C., Long, G. V., Brady, B., Dutriaux, C., Maio, M., Mortier, L.,… Ascierto, P.
671 A. (2015). Nivolumab in previously untreated melanoma without BRAF
672 mutation. *New England Journal of Medicine*, *372*(4), 320–330.
673 https ://doi.org/10.1056/NEJMo a1412082
674
675 Sandru, A., Voinea, S., Panaitescu, E., & Blidaru, A. (2014). Survival rates of patients
676 with metastatic malignant melanoma. *Journal of Medicine and Life*, *7*(4), 572–
677 576.
678
679 Sasaoka, N., Sakamoto, M., Kanemori, S., Kan, M., Tsukano, C., Takemoto, Y., &
680 Kakizuka, A. (2014). Long-term oral administration of hop flower extracts
681 mitigates Alzheimer phenotypes in mice. *PLoS ONE*, *9*(1), e87185.
682 https ://doi.org/10.1371/journ al.pone.0087185
683
684 Schadendorf, D., van Akkooi, A. C. J., Berking, C., Griewank, K. G., Gutzmer, R.,
685 Hauschild, A., … Ugurel, S. (2018). Melanoma. *Lancet*, *392*(10151), 971–984.
686 https ://doi.org/10.1016/S0140-6736(18)31559-9
687
688 Scifinder (2017). Chemical Abstracts Service: Columbus, OH; RN518-82-1, RN 521-
689 61-9, RN 555-60-2 (accessed Feb 18, 2017); calculated using ACD/Labs
690 software, version 11.02; ACD/Labs 1994–2018.
691
692 Siegel, R. L., Miller, K. D., & Jemal, A. (2018). Cancer statistics, 2018. *CA: A Cancer*
693 *Journal for Clinicians*, *68*(1), 7–30. https ://doi.org/10.3322/caac.21442
694
695 Singh, D., Banerji, A. K., Dwarakanath, B. S., Tripathi, R. P., Gupta, J. P., Mathew, T.
696 L., … Jain, V. (2005). Optimizing cancer radiotherapy with 2-deoxy-D-
697 glucose. *Strahlentherapie Und Onkologie*,*181*(8), 507–514.
698 https ://doi.org/10.1007/s00066-005-1320-z
699
700 Škrtić, M., Sriskanthadevan, S., Jhas, B., Gebbia, M., Wang, X.,Wang, Z., …
701 Schimmer, A. D. (2011). Inhibition of mitochondrial translation as a
702 therapeutic strategy for human acute myeloid leukemia. *Cancer Cell*, *20*(5),
703 674–688. https ://doi.org/10.1016/j.ccr.2011.10.015
704

Su, Y. T., Chang, H. L., Shyue, S. K., & Hsu, S. L. (2005). Emodin induces apoptosis in human lung adenocarcinoma cells through a reactive oxygen species-dependent mitochondrial signaling pathway. *Biochemical Pharmacology*, *70*(2), 229–241. https ://doi.org/10.1016/j.bcp.2005.04.026

Summers, K. E., & Gibbons, I. R. (1971). Adenosine triphosphate-induced sliding of tubules in trypsin-treated flagella of sea-urchin sperm. *Proceedings of the National Academy of Sciences*, *68*(12), 3092–3096. https ://doi.org/10.1073/pnas.68.12.3092

Tsang, R. Y., Al-Fayea, T., & Au, H. J. (2009). Cisplatin overdose: Toxicities and management. *Drug Safety*, *32*(12), 1109–1122. https://doi.org/10.2165/11316640-00000 0000-00000

Ubbink-Kok, T., Anderson, J. A., & Konings, W. N. (1986). Inhibition of electron transfer and uncoupling effects by emodin and emodinanthrone in Escherichia coli. *Antimicrobial Agents and Chemotherapy*, *30*(1), 147–151. https ://doi.org/10.1128/AAC.30.1.147

Vander Heiden, M. G. (2011). Targeting cancer metabolism: A therapeutic window opens. *Nature Reviews Drug Discovery*, *10*(9), 671–684. https ://doi.org/10.1038/nrd3504

Vernieri, C., Casola, S., Foiani, M., Pietrantonio, F., de Braud, F., & Longo, V. (2016). Targeting Cancer Metabolism: Dietary and Pharmacologic Interventions. *Cancer Discovery*, *6*(12), 1315–1333. https ://doi.org/10.1158/2159-8290.CD-16-0615

Warburg, O. (1956). On the origin of cancer cells. *Science*, *123*(3191), 309–314.

Warburg, O., Posener, K., & Negelein, E. (1924). Uber den Stoffwechsel der Carcinomzelle. *Biochemische Zeitschrift*, *152*, 309–344.

Weinberg, S. E., & Chandel, N. S. (2015). Targeting mitochondria metabolism for cancer therapy. *Nature Chemical Biology*, *11*(1), 9–15. https ://doi.org/10.1038/nchem bio.1712

Yin, M., Zhou, J., Gorak, E. J., & Quddus, F. (2013). Metformin is associated with survival benefit in cancer patients with concurrent type 2 diabetes: A systematic review and meta-analysis. *The Oncologist*, *18*(12), 1248–1255. https ://doi.org/10.1634/theon colog ist.2013-0111

Zhang, H., Li, C., Kwok, S. T., Zhang, Q. W., & Chan, S. W. (2013). A review of the pharmacological effects of the dried root of *Polygonum cuspidatum* (Hu Zhang) and its constituents. *Evidence-Based Complementary and Alternative Medicine*, 208349. https ://doi.org/10.1155/2013/208349

Zhang, Z. J., Bi, Y., Li, S., Zhang, Q., Zhao, G., Guo, Y., & Song, Q.(2014). Reduced risk of lung cancer with metformin therapy in diabetic patients: A systematic review and meta-analysis. *American Journal of Epidemiology*, *180*(1), 11–14. https ://doi.org/10.1093/aje/kwu124

FIGURE LEGENDS

FIGURE 1

A plant extract from rhizomes of *Polygonum cuspidatum* preferentially decreases cellular adenosine triphosphate (ATP) levels in B16F10 cells but not MEFs.

(a) The proliferative propensities of B16F10 and MEF cell lines were compared by mean values of total cell numbers at the respective time points. *n* = 3 at each point. (b and c) Analyses of energy metabolism. Extra cellular acidification rate (ECAR) (b) and oxygen consumption rate (OCR) (c) were measured using Seahorse XF96 Analyzer (Agilent). ECAR of glycolysis: (ECAR of basic state) − (ECAR after treatment with 100 mM of 2 - deoxyglucose). OCR of mitochondrial respiration: (OCR of basic state) − (OCR after the treatment with respiration inhibitors, rotenone and antimycin (3 μM each)). B16F10: *n* = 5, MEF: *n* = 3.

(d) Two cell lines were stained with tetramethylrhodamine methyl ester (TMRM), and the mitochondrial membrane potential (MMP) in the basic state for each cell line was compared by measuring the intensity of fluorescence using microscopic analysis. Fluorescence intensities are presented as mean values of respective cells in each cell

795 line; B16F10, *n* = 22. MEF, *n* = 28.

796 (e) ATPase activities of whole cell lysates from B16F10 and MEF cells were measured

797 by a modified molybdate assay. Each cell lysate was diluted to the same concentration

798 of total protein, and ATP hydrolysis reactions were carried out. The results are

799 presented as means of three ATP hydrolysis reactions.

800 (a - e) Error bars indicate standard deviations. (b–e) *$p < 0.05$, ***$p < 0.005$, by

801 Student's *t* test.

802 (f) The two cell lines, B16F10 and MEF, were cultured with each plant extract at 100

803 μg/ml for 6 hr (A: *Rhizoma Polygonum cuspidatum*, B: *Rhizoma Cortex periplocae*, C:

804 *Fructu Cucurbitae moschatae*, D: *Flos Chrysanthem*, E: *Semen Lepidii*) and subjected

805 to luciferase - based ATP quantifications. The

806 results were normalized by the protein amount in each well and showed as averages

807 and standard deviations. *$p < 0.05$, ***$p < 0.005$, (B16F10, vs. DMSO), †$p < 0.05$, ††p

808 < 0.01 (MEF, vs. DMSO), by Dunnett's test. N.S., not significant

809

810 **FIGURE 2**

811 **Emodin is the responsible ingredient in the RPC extract.**

812 (a) Schematic flow of the polarity - based fractionations of the extract from rhizome of

Polygonum cuspidatum. The bioactivities that lowered adenosine triphosphate (ATP) levels in cells were found in fractions F2 and F2 - 1, as shown in bold characters. (b and c) Luciferase - based ATP quantifications. Before the measurements, B16F10 cells and MEF cells were treated with DMSO, #1 (crude, lot.1), #2 (crude, lot.2), #2 - F1 or #2 - F2, for 6 hr in (b). In (c), cells were cultured with the indicated fractions purified from #2 (crude, lot.2), F2, F2 - 1, F2 - 2, F2 - 3 or DMSO, for 6 hr. The results show means with standard deviations. ***$p < 0.005$. (B16F10, vs. DMSO), ††$p < 0.01$, †††$p < 0.005$ (MEF, vs. DMSO), by Dunnett's test. N.S., not significant. (d and e) Reverse - phase HPLC analysis of F2 - 1 from the SPE and commercially available standard compounds, emodin and physcion. Acetonitrile - dissolved samples were applied to a Mightysil RP - 18 GP 150–4.6 (5 μm) column and eluted with a linear gradient of acetonitrile, 40% to 90% for 30 min, in water with 0.1% trifluoroacetic acid (TFA).

(d) Chromatograms of each sample at 254 nm are shown. (e) Ultraviolet –visible absorption spectra of each sample (210 nm−600 nm) are shown.

(f and g) 1H - NMR (DMSO - d6) analysis of F2 - 1 and commercially available standards, emodin and physcion. (h) Chemical structures of the anthraquinones, emodin and physcion.

(i) Luciferase - based ATP quantifications. B16F10 cells and MEF cells were treated with DMSO or standard chemicals (emodin (8 μg/ml) or emodin (8 μg/ml) + physcion (2.24 μg/ml) (1:0.28 molar ratio)), for 6 hr, followed by ATP quantifications in each lysate. The result shows the average of four wells, and error bars indicate standard deviations. ***$p < 0.005$ (versus DMSO), by Dunnett's test. N.S., not significant

FIGURE 3

Emodin suppresses cell proliferation of B16F10 cells in vitro and in vivo.

(a and b) B16F10 cells and MEF cells were treated with or without the indicated concentrations of emodin for 24 hr followed by a cell proliferation assay using a trypan blue dye - exclusion test (left), and 6 - hr treatment was carried out for an evaluation of adenosine triphosphate (ATP) levels using a luciferase assay (right). Each result shows the average of three independent trials, and error bars indicate standard errors. Statistical analyses were carried out using total cell numbers. *$p < 0.05$, ***$p < 0.005$ (B16F10, vs. DMSO), †$p < 0.05$, ††$p < 0.005$ (MEF, vs. DMSO), by Dunnett's test. N.S., not significant.

(c) Western blot analyses using whole cell lysates of each cell line. Before lysis, each cell line was treated with DMSO, emodin (8 or 16 μg/ml) or cisplatin (CDDP) (30 or 100

μM) for 6 hr. Phosphorylation of AMPK at threonine 172 and expression levels of AMPKα, p53 and actin, were evaluated.

(d) B16F10 cells (left) and MEF cells (right) were cultured with DMSO, emodin (4 or 8 μg/ml) or CDDP (1 or 2 μM), for three days. At the respective time point days 0, 1, 2 and 3, total cell numbers per well were recorded. Each result shows the average of three independent trials, and error bars indicate the standard error. The *p* value indicates the statistical result of Dunnett's test (vs. DMSO at Day 3).

(e) Schematic drawing of the experimental design for the tumor growth assay. C57BL/6N (female) mice were transplanted with B16F10 cells (2 × 105 cells in PBS), and intraperitoneal administrations of vehicle or emodin (50 mg/kg body weight) were initiated following day.

(f) Monitoring tumor growth in mice. The result shows each tumor volume per mouse, with the horizontal bar indicating the average, at Days 8, 10 and 12. *$p < 0.05$, **$p < 0.01$ (Vehicle vs. EMO), by Student's *t* test

FIGURE 4

Emodin functions as a mitochondrial uncoupler.

(a) Cell lines were cultured on collagen - coated glass - bottom dishes for

867 approximately 24 hr, and medium was replaced by fluorescent dye - containing media
868 (50 nM of TMRM, 1 μg/ml of Hoechst 33342, phenol red(−)) followed by incubation at
869 37℃ for 30 min. The fluorescence images representing MMPs, before and after the
870 addition of emodin (8 μg/ml, final),were captured, and each fluorescence intensity per
871 cell was quantified using MetaMorph (Molecular Devices). ***p < 0.005 (B16F10, vs. 0
872 min),†††p < 0.005 (MEF, vs. 0 min), by Dunnett's test.
873 (b) In parallel, dishes with each respective cell line were subjected to a preliminary
874 treatment
875 with DMSO or emodin (8 μg/ml) for 24 hr, and the respective intensity of TMRM was
876 compared using the same analysis as in (a) to yield the result at 24 hr. The results are
877 presented as box - and - whisker plots. ***p < 0.005 (vs. DMSO) by Student's t test.
878 (c and d) The effect of emodin on mitochondrial respiration was evaluated by Seahorse
879 XF96 Analyzer. Cells were cultured for approximately 24 hr, and growth medium was
880 replaced by XF RPMI 1640 - based medium (bicarbonate - free, Seahorse). In (c),
881 measurements of the OCR were carried out with the following initial injections: emodin
882 (8 μg/ml, final), CCCP (5 μM, final) or rotenone (0.3 μM: final). The second injection
883 was a mixture of complex Ⅰ inhibitors (rotenone + antimycin, 3 μM each, final).
884 Respective results represent the average of five wells, and error bars indicate standard

deviations. In (d), the first injection was oligomycin (3 μM: final), which was followed by the second injections: emodin (8 μg/ml, final) or CCCP (5 μM, final); a third injection consisted of a mixture of complex Ⅰ inhibitors (rotenone + antimycin, 3 μM each, final). Each result represents the average of 5 wells, and error bars indicate standard deviations.

(e) Calculated values from the database (SciFinder), of pKa and logP.

(f) MMPs of two cell lines, before and after the addition of emodin, uncouplers (CCCP, FCCP or DNP) or CDDP, were evaluated using TMRM (50 nM) and Hoechst 33342 (1 μg/ml). Scale bar, 50 μm. In this figure, the MPP brightness of MEF cells was enhanced to clarify the differences before and after the injection of uncouplers. The unenhanced images are shown in Figure S7.

(g and h) Cell lines were treated with DMSO, emodin, uncouplers (CCCP, FCCP or DNP) or CDDP, for 6 hr followed by luciferase - based ATP quantification (g), and in the case of 24 - hr treatments, cells were subjected to a trypan blue dye - exclusion test (h). Each vertical bar indicates the average of three wells, and error bars indicate standard deviations. *$p < 0.05$, ***$p < 0.005$ (B16F10, vs. DMSO), †$p < 0.05$, †††$p < 0.005$ (MEF, vs. DMSO), by Dunnett's test.

(i and j) Cell lines were treated with DMSO or complex Ⅰ inhibitors (rotenone or

903 metformin) for 6 hr, followed by luciferase - based ATP quantification (i), and in case of
904 the 24 - hr assay, total and living cell numbers were assessed by a trypan blue dye -
905 exclusion test (j). Results indicate mean values, and error bars indicate standard
906 deviations. ***$p < 0.005$ (B16F10, vs. DMSO), †††$p < 0.005$. (MEF, vs. DMSO), by
907 Dunnett's test. Statistical analyses were carried out using total cell numbers in (h, j)
908
909 **FIGURE 5**
910 **Glycolytic reserve of B16F10 cells is poor compared with that of MEF cells.**
911 (a) B16F10 and MEF cells were cultured in 24 - well plates for approximately 24 hr,
912 and the growth medium was replaced by fresh medium containing DMSO, emodin (8
913 μg/ml), CCCP (5 μM), FCCP (3.5 nM), DNP (150 μM) or CDDP (30 μM), respectively.
914 After incubation for 4 hr, respective culture media were collected, and glucose
915 concentrations were measured by the glucose CII test (Wako). The results were
916 normalized to the attached cell number for each well. The data represent averages of
917 four wells, and error bars indicate standard deviations. ***$p < 0.005$ (B16F10, vs.
918 DMSO), †††$p < 0.005$ (MEF, vs. DMSO), by Dunnett's test. N.S., not significant.
919 (b) CCCP’s effect on glycolysis was evaluated by monitoring ECAR using Seahorse
920 XF96 Analyzer. Approximately 24 hr after plating, cells were treated with the indicated

concentrations of CCCP (2.5 or 5 μM, final) for the initial injections, followed by a second injection of 2 - DG (100 mM, final). Results are shown as ECAR per 1 × 104 cells, which represent the mean values of four wells. Error bars show standard deviations.

(c) Uncouplers' effects on glycolysis were evaluated by monitoring ECAR using Seahorse XF96 Analyzer. Two cell lines were treated with the indicated concentrations of mitochondrial uncouplers (CCCP, FCCP, DNP), CDDP (30 μM) or DMSO for the initial injections, followed by a second injection of 2 - DG (100 mM, final). Results are shown as ECAR per 1 × 104 cells, which represent the mean values. Error bars show standard deviations.

(d) B16F10 and MEF cells were treated with DMSO or emodin (8 μg/ml) for 6 hr, with the indicated concentrations of glucose (0, 50, 100 or 200 mg/dl) (in correct, this medium included FBS - contained glucose), and were subjected to cellular adenosine triphosphate (ATP) quantification using the luciferase assay. Each value for the luciferase assay was normalized by the protein amount in each well. The data represent mean values, and error bars indicate standard deviations. *$p < 0.05$, ***$p < 0.005$, by Student's *t* test (vs. DMSO). N.S., not significant.

(e) A model of energy balance in each cell line, under the two different conditions. In basic conditions, B16F10 cells produce and consume a large amount of ATP. In the presence of a mitochondrial uncoupler, this cell line cannot maintain its energy state by relying on glycolysis, because of the poor glycolytic reserve. In contrast, because the turnover of ATP in MEF cells is slow and basal glycolysis is very low, their glycolytic reserve can compensate for the energy depletion brought about by mitochondrial uncoupling.

FIGURE 1

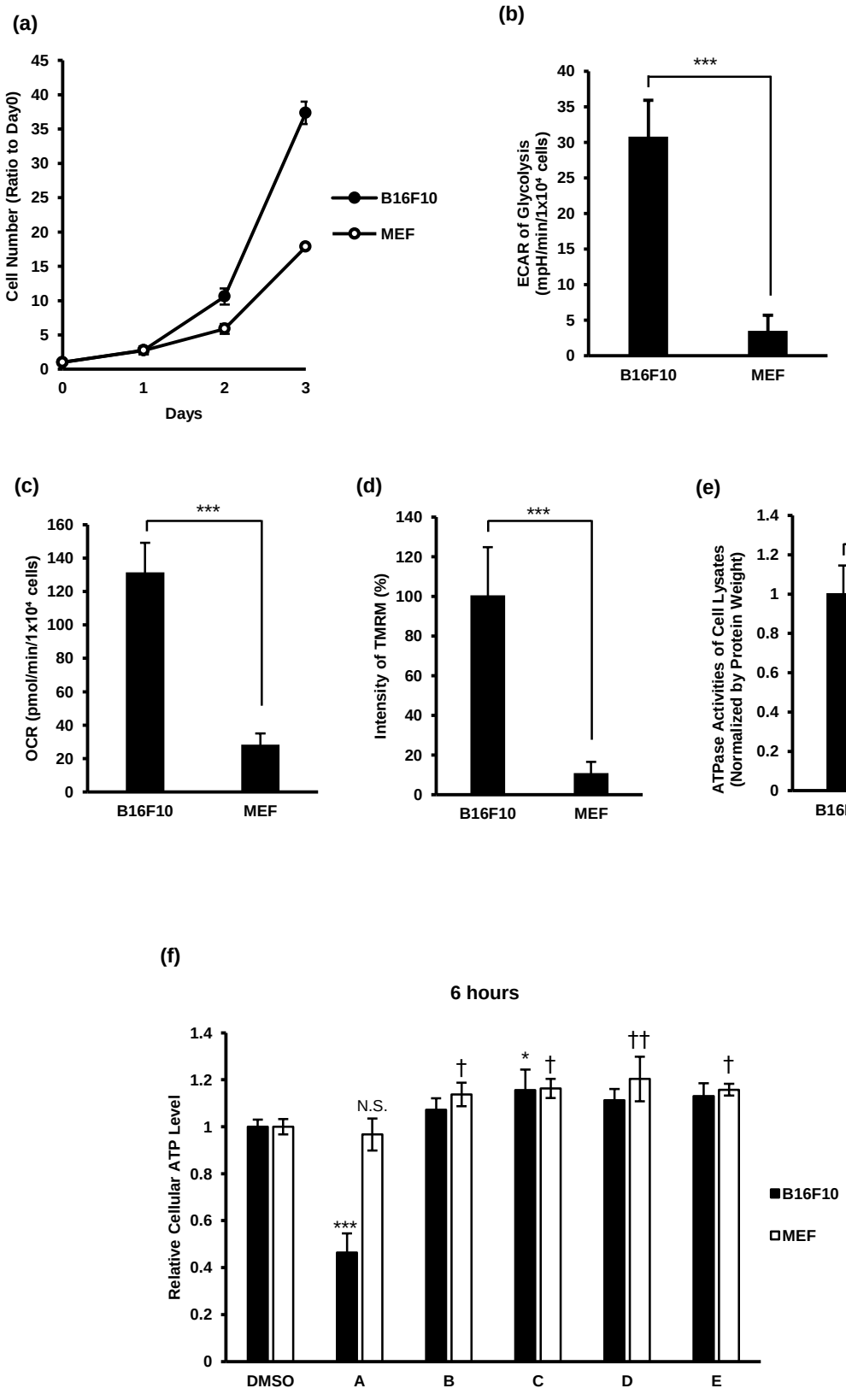

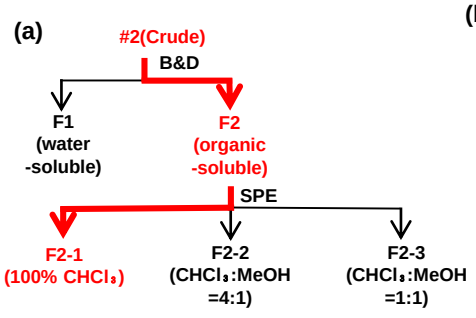

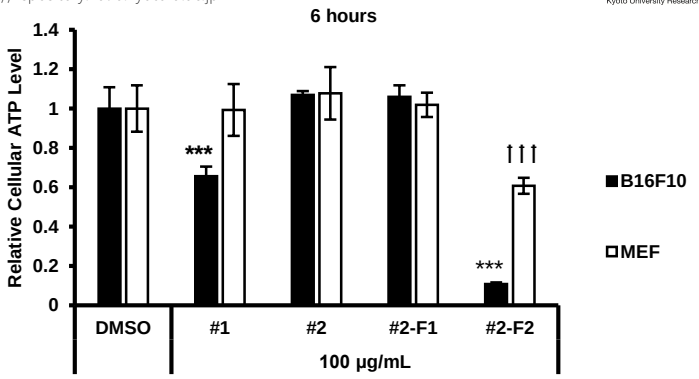

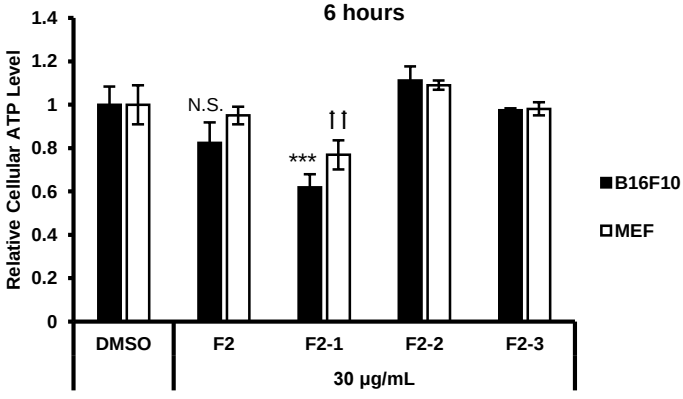

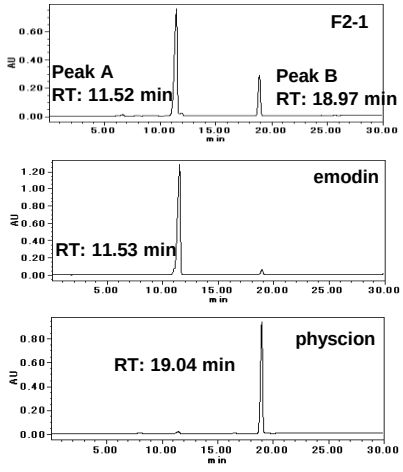

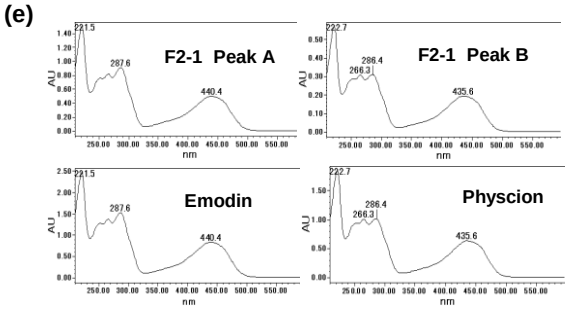

(g)

Commercially available standards (^{1}H-NMR)(DMSO-d_6)

Atom	Emodin (ppm)	Physcion (ppm)
OH - 1/8	12.03 (brs) / 12.09 (brs)	12.11 (brs) / 12.11 (brs)
H - 7	7.16 (brs)	7.22 (brs)
H - 5	7.48 (brs)	7.54 (brs)
H - 4	7.10 (d, J = 2.6 Hz)	7.21 (d, J = 2.3 Hz)
H - 2	6.57 (d, J = 2.6 Hz)	6.89 (d, J = 2.3 Hz)
H (Me)	2.41 (s)	2.44 (s)
H (MeO)	-	3.94 (s)

(f)

F2-1 (^{1}H-NMR)(DMSOd_6)

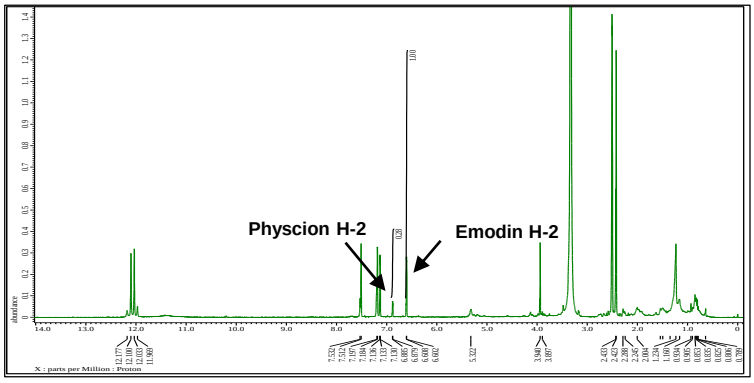

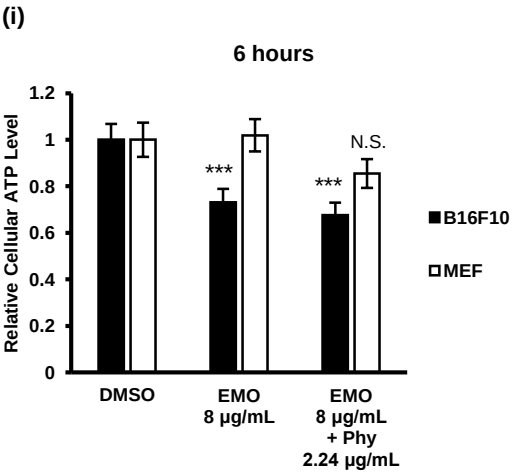

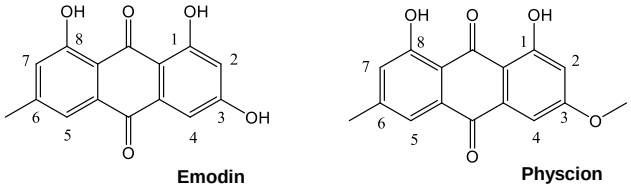

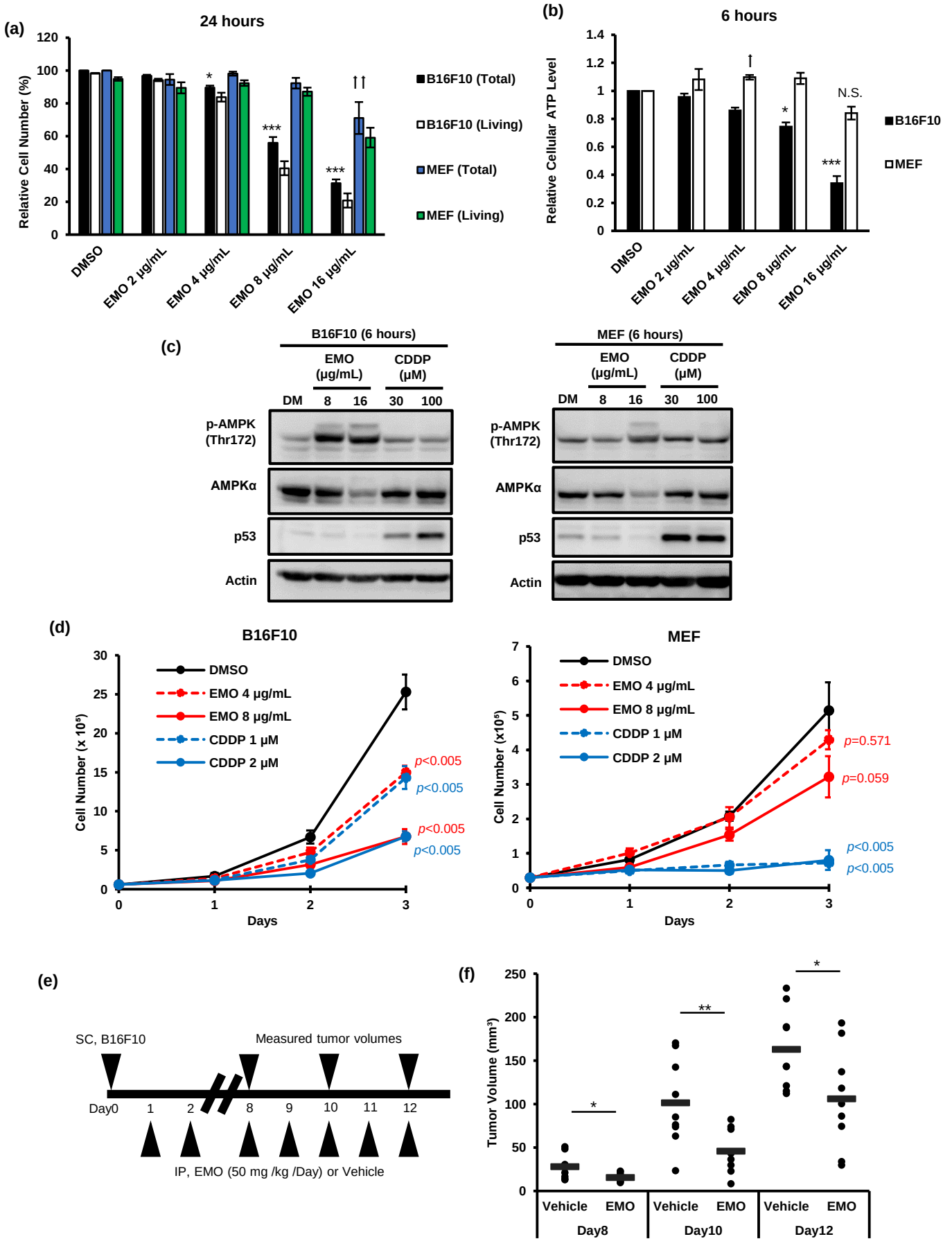

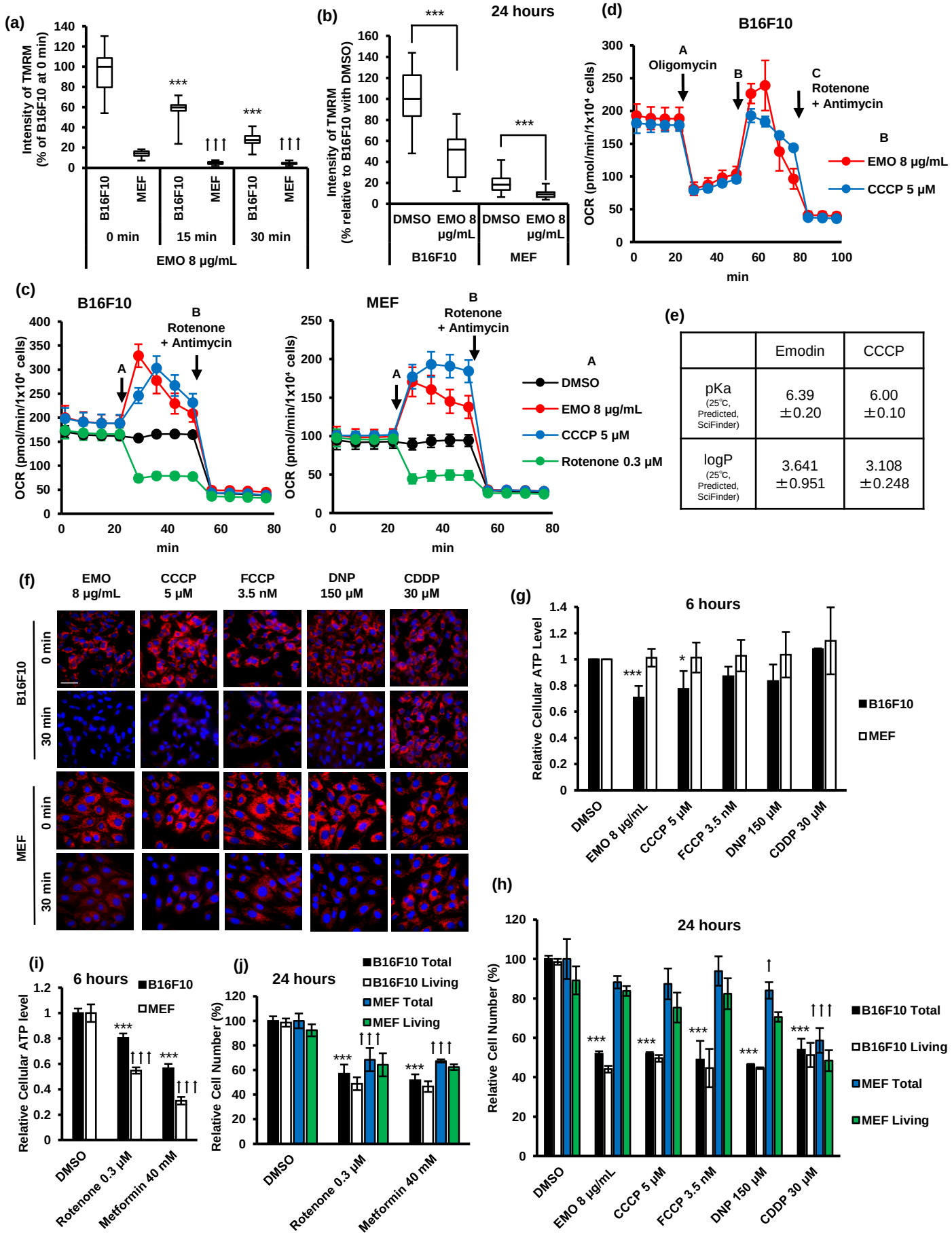

	Emodin	CCCP
pKa (25℃, Predicted, SciFinder)	6.39 ±0.20	6.00 ±0.10
logP (25℃, Predicted, SciFinder)	3.641 ±0.951	3.108 ±0.248

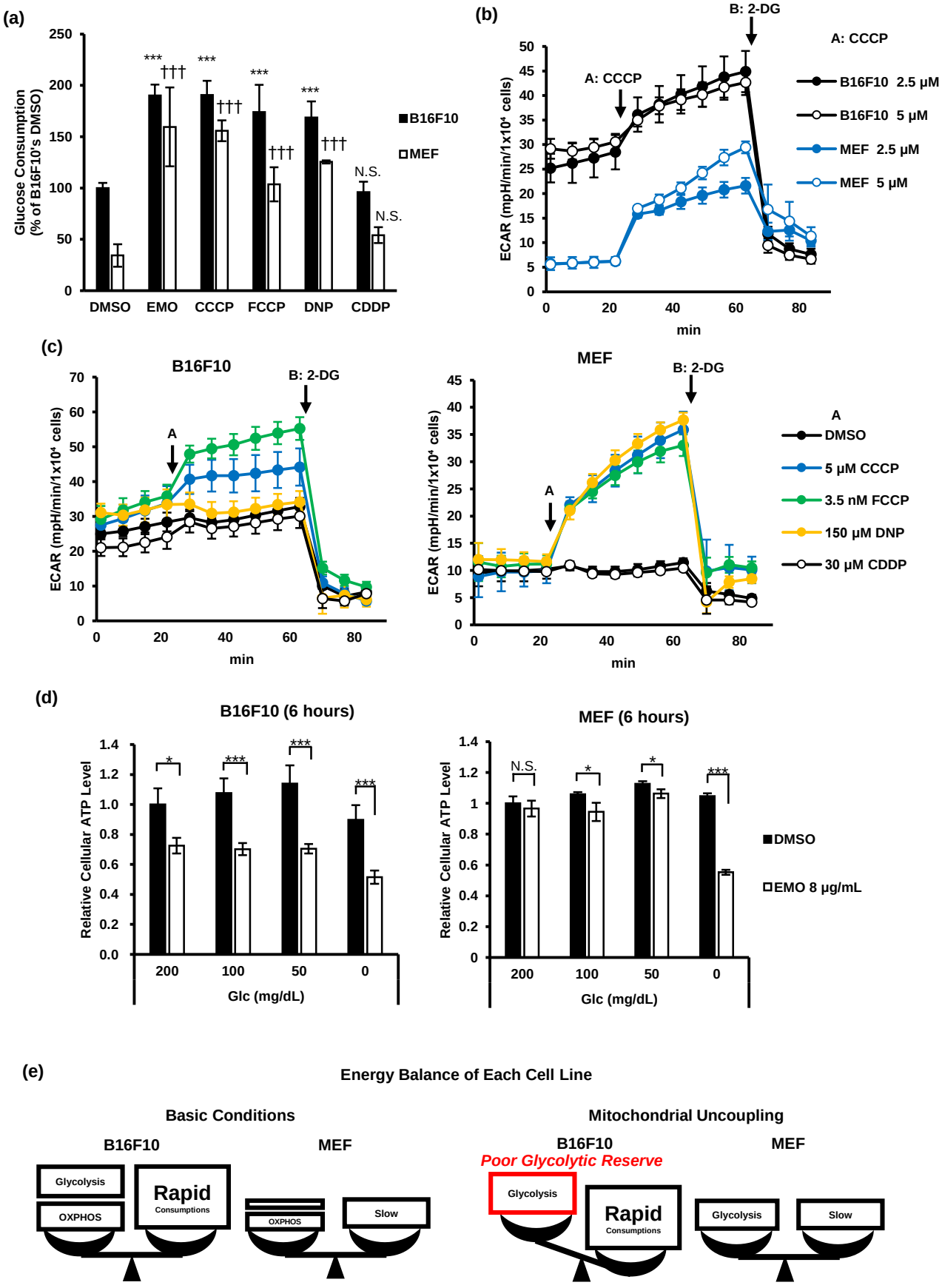

Supporting Information Figures

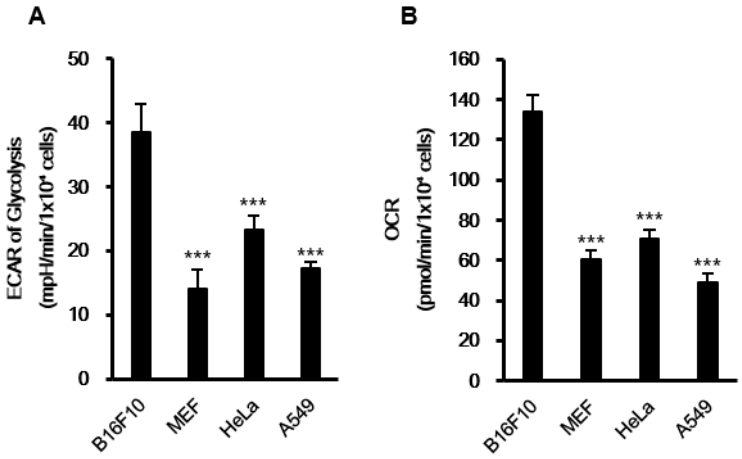

Figure S1 – HeLa and A549 cells exhibited lower glycolysis and oxygen consumption rate compared to B16F10 cells.

(A)(B) Analysis of energy metabolism. ECAR (A) and OCR (B) were measured by a XF96 system (Seahorse). ECAR of glycolysis: (ECAR of basic state) − (ECAR after treatment with 100 mM of 2-deoxyglucose). OCR of mitochondrial respiration: (OCR of basic state) − (OCR after the treatment with respiration inhibitors, rotenone and antimycin (3 μM each)). B16F10: n=3, MEF: n=3, HeLa: n=3, A549: n=5. *** $p < 0.005$ (vs. B16F10) by Dunnett's test.

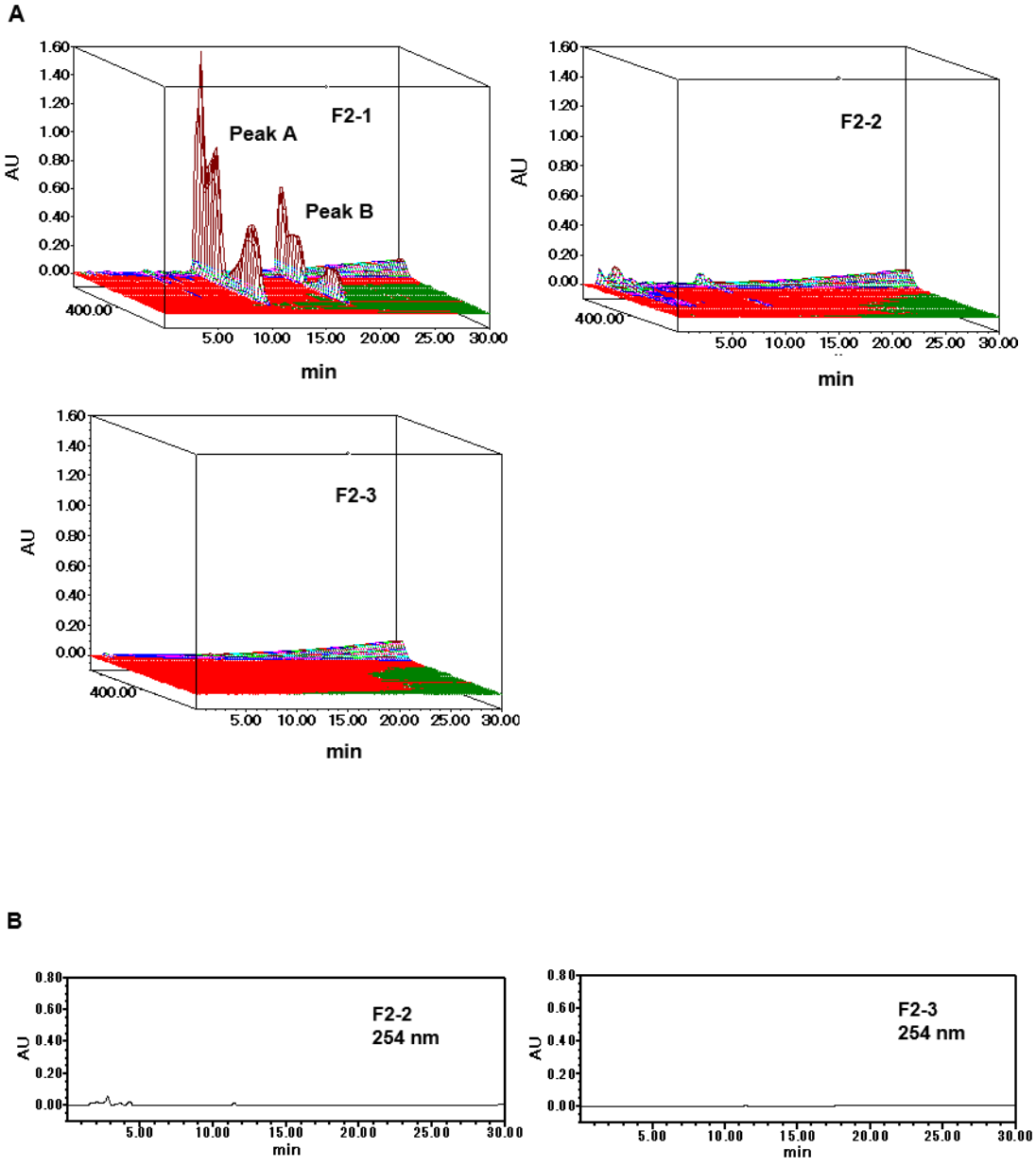

Figure S2 – F2-2 and F2-3 have no obvious peaks like peak A and B in F2-1.

(A) Fractions after SPE, F2-1, F2-2 and F2-3, were applied to a reverse-phase HPLC column. The results of 210- 600 nm are shown as three-dimensional chromatograms.

(B) The chromatograms of F2-2 and F2-3, at 254 nm.

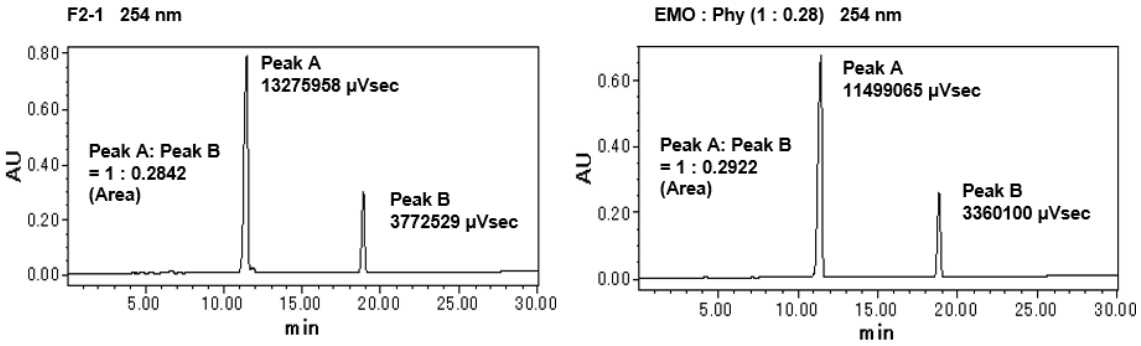

Figure S3 - The area ratio of the two peaks in F2-1 and the mixed sample (emodin (EMO) and physcion (Phy), 1: 0.28 molar ratio) were very close.

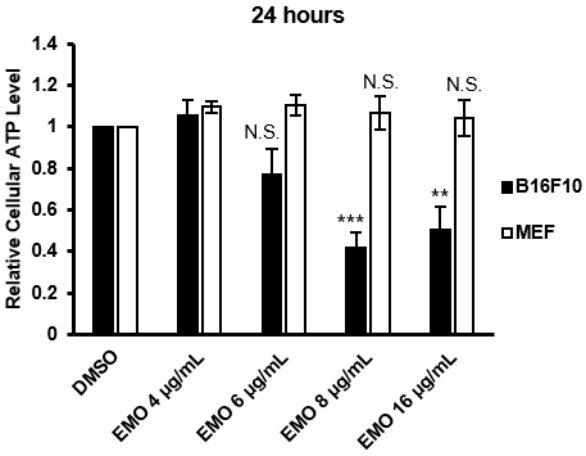

Figure S4 – Emodin-induced cellular ATP reductions in B16F10 are also evident after 24 hours treatment at concentrations of 6 (not significant), 8, and 16 μg/mL. ** p< 0.01, *** p< 0.005 (vs. DMSO), by Dunnett's test. N.S., not significant.

,

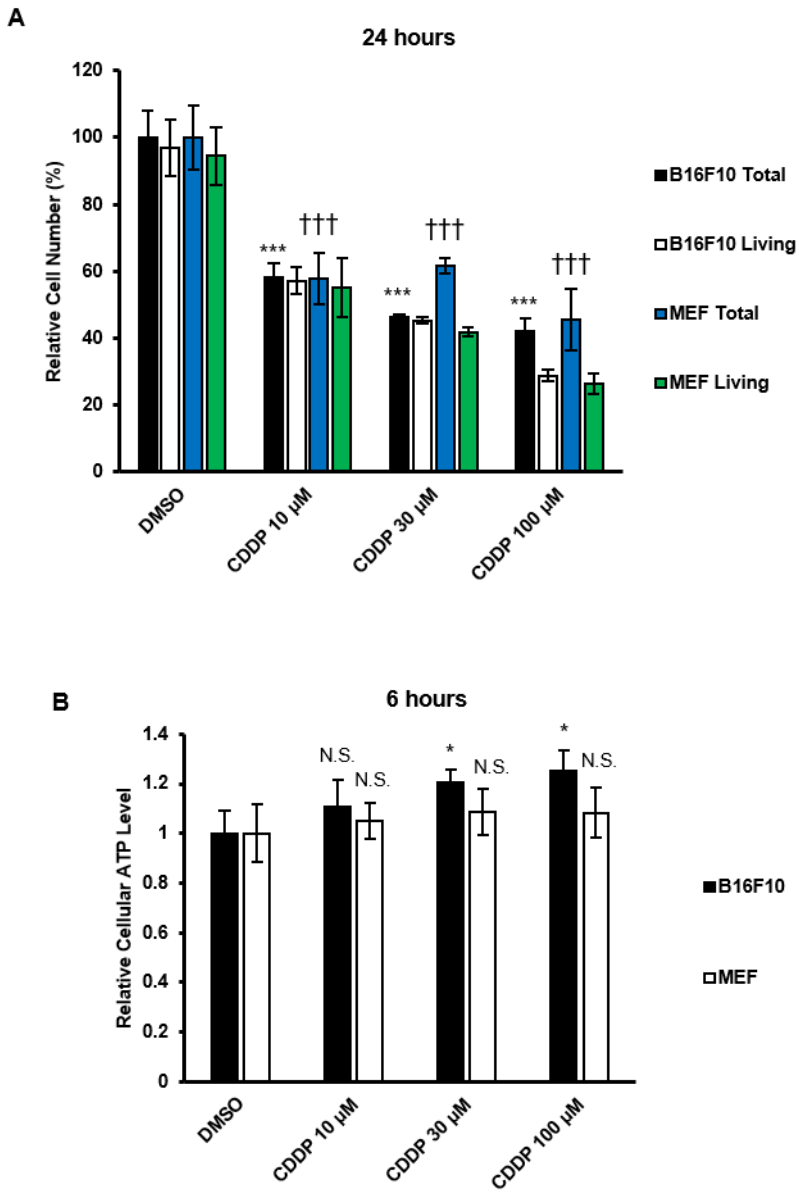

Figure S5 – CDDP suppresses cell proliferation of B16F10 and MEF equally, but does not lower cellular ATP levels.

(A) Trypan blue dye exclusion test after treatment with DMSO or CDDP (10, 30, or 100 μM), for 24 hours. Results indicate averages and standard deviations. Statistical analyses were performed using total cell numbers. *** p< 0.005 (B16F10, vs. DMSO), ††† p< 0.005 (MEF, vs. DMSO), by Dunnett's test.

(B) Luciferase-based ATP quantification (ToyoB-net) after treatment with DMSO or CDDP (10, 30, or 100 μM) for 6 hours. Results indicate averages and standard deviations. * p< 0.05 (vs. DMSO) by Dunnett's test. N.S., not significant.

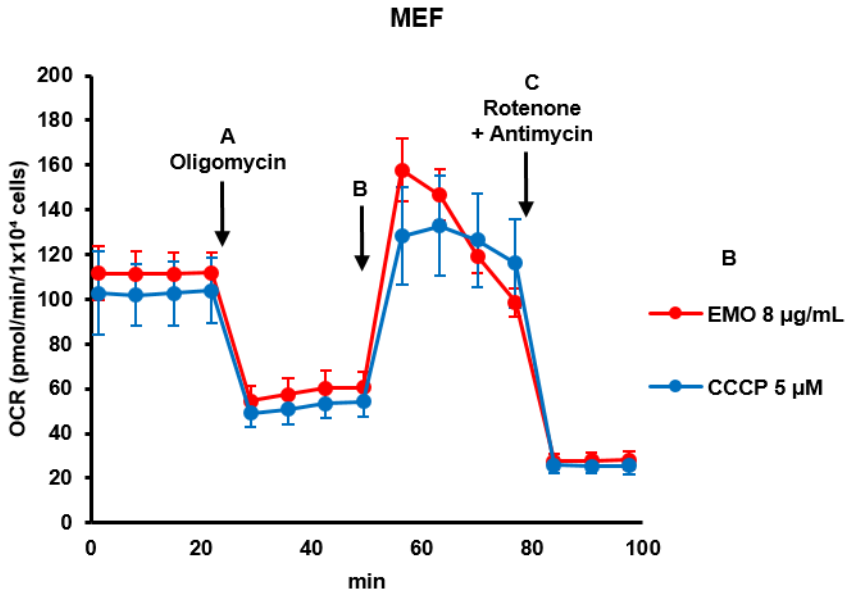

Figure S6 – MEF cells also showed stimulated respiration after addition of emodin or CCCP, even in the ATP synthase-inhibited state.

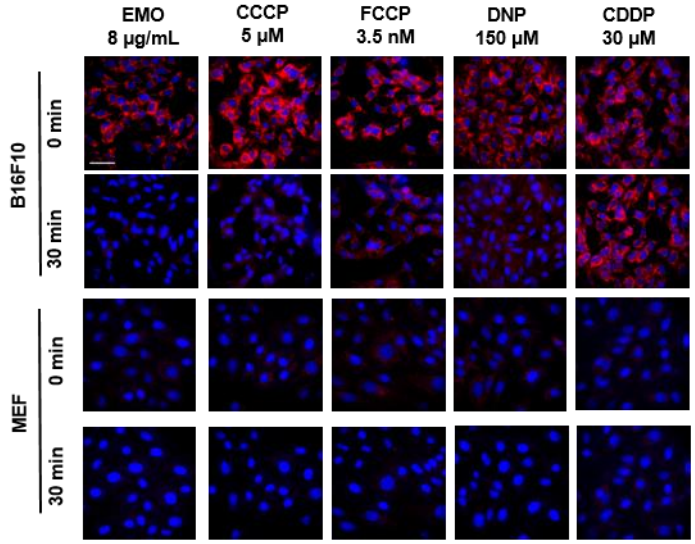

Figure S7 – The MMP of MEF cells was much lower than the MMP of B16F10 cells in the basic state. This figure is based on the same photos of Figure 4f, without enhancement. Scale bar, 50 μm.

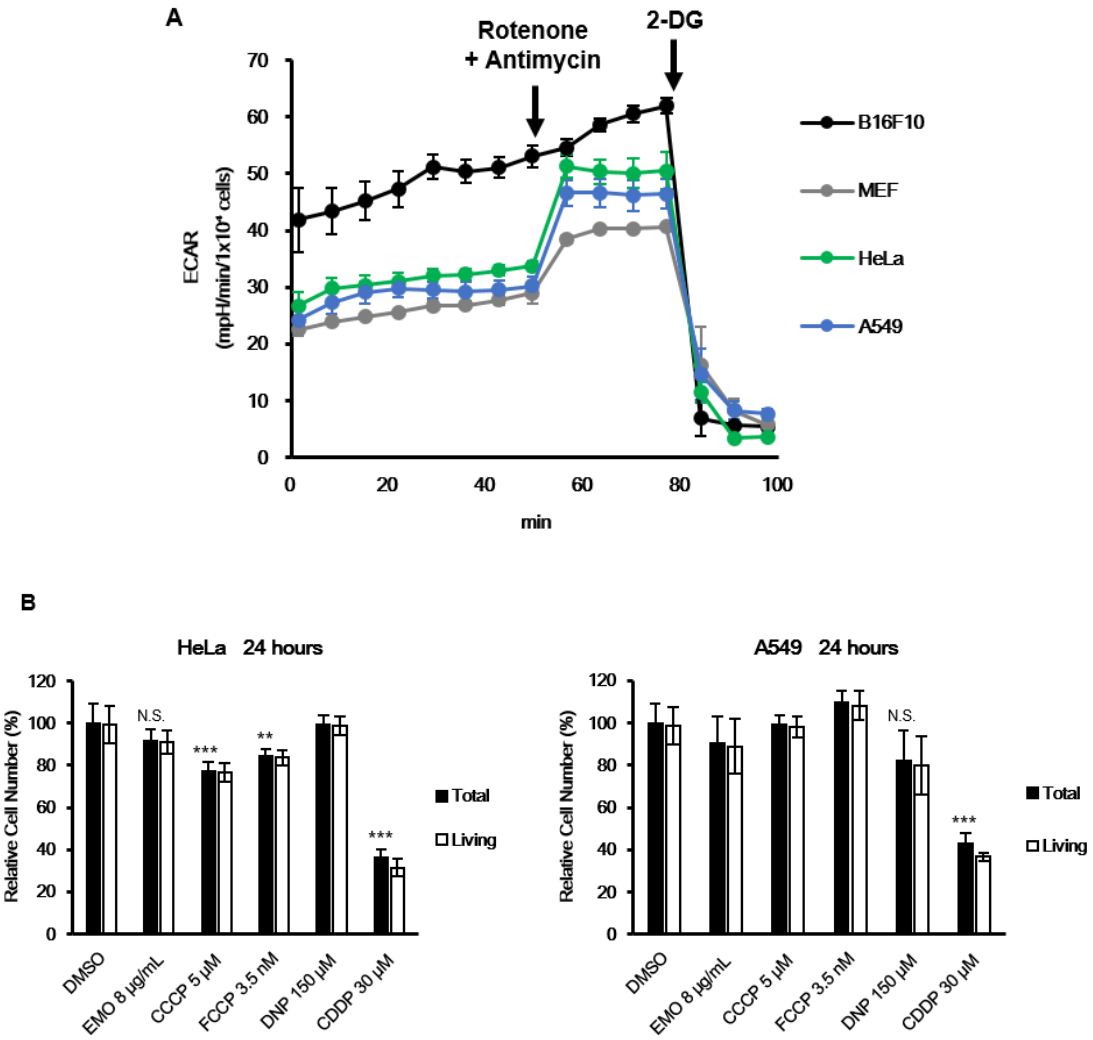

Figure S8 – HeLa and A549 cells have more glycolytic reserve than B16F10 cells.

(A) ECAR of four cell lines were analyzed by XF96 system (Seahorse).
Rotenone + Antimycin: 3 μM each. 2-DG: 100 mM. B16F10: n=3, MEF: n=3, HeLa: n=3, A549: n=5. Growth media were followings; B16F10 and MEF cells: RPMI1640. HeLa and A549: DMEM (High glucose). For the experiments using XF96 system, we used XF system-specified media (Seahorse). All experiments were performed with 10% fetal bovine serum.

(B) HeLa and A549 cells were treated with DMSO, emodin, uncouplers (CCCP, FCCP, or DNP), or CDDP, for 24 hours, and cells were subjected to a trypan blue dye-exclusion test. Results indicate averages and standard deviations of three wells. Statistical analyses were performed using total cell numbers. ** $p < 0.01$, *** $p < 0.005$ (vs. DMSO), by Dunnett's test. N.S., not significant.

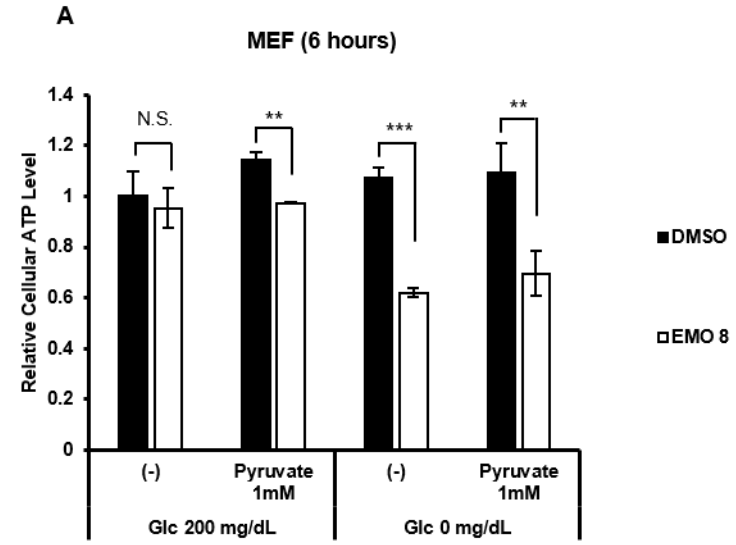

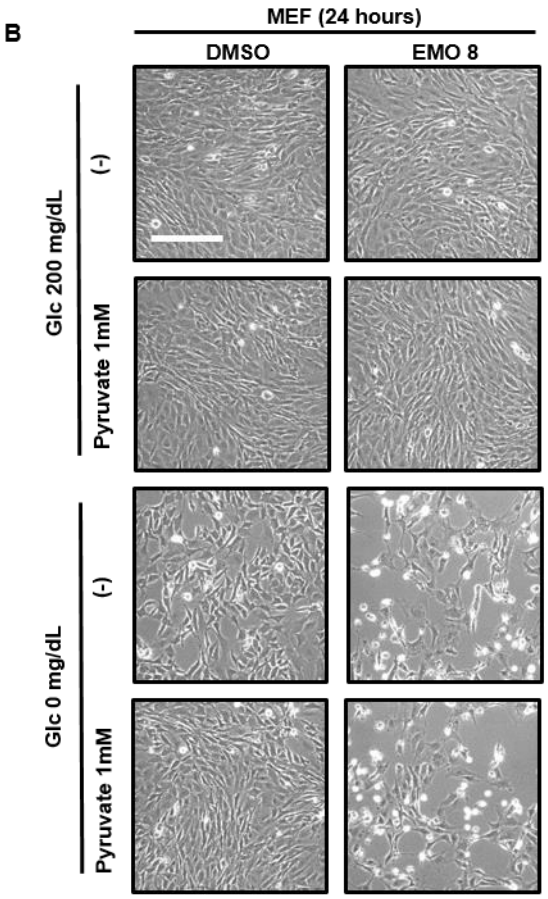

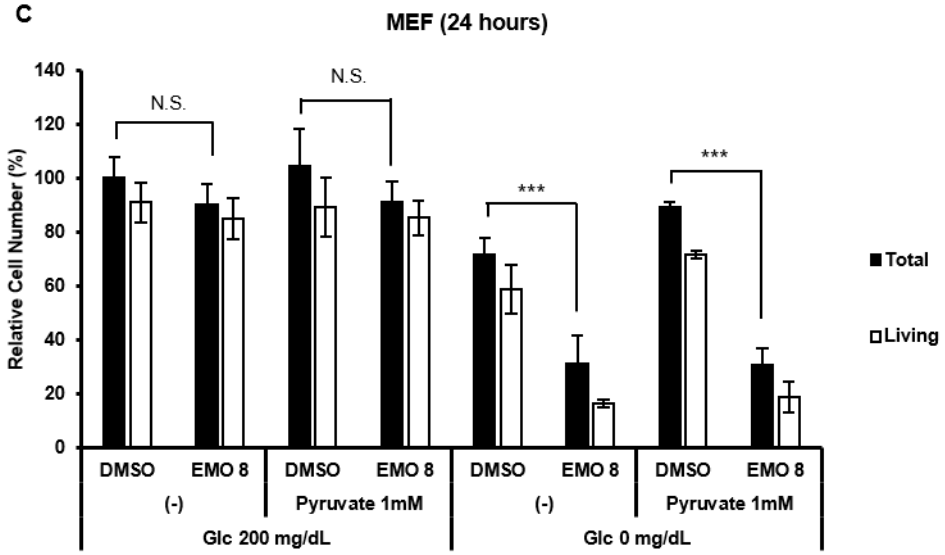

Figure S9 - MEF cells avoid emodin-induced perturbations, such as energy depletion and reduced proliferation, by virtue of an intact glycolytic reserve.

(A) Luciferase-based ATP quantification after 6 hours culture with or without emodin (8 μg/mL), with or without glucose (200 mg/dL). Results indicate averages and standard deviations of three wells. ** $p < 0.01$, *** $p < 0.005$ (vs. DMSO), by Student's *t* test. N.S., not significant.

(B)(C) ~~Trypan blue dye exclusion test (A) and photos (B)~~ Photos (B) and trypan blue dye exclusion test (C) after culture with or without emodin (8 μg/mL), for 24 hours, with or without 200 mg/dL of glucose. Scale bar, 250 μm. Results indicate averages and standard deviations of three wells. *** $p < 0.005$ (vs. DMSO) by Student's *t* test. N.S., not significant. The statistical analyses of (C) were performed using total cell numbers. In correct, the medium named as Glc 0 mg/dL included FBS-contained glucose.

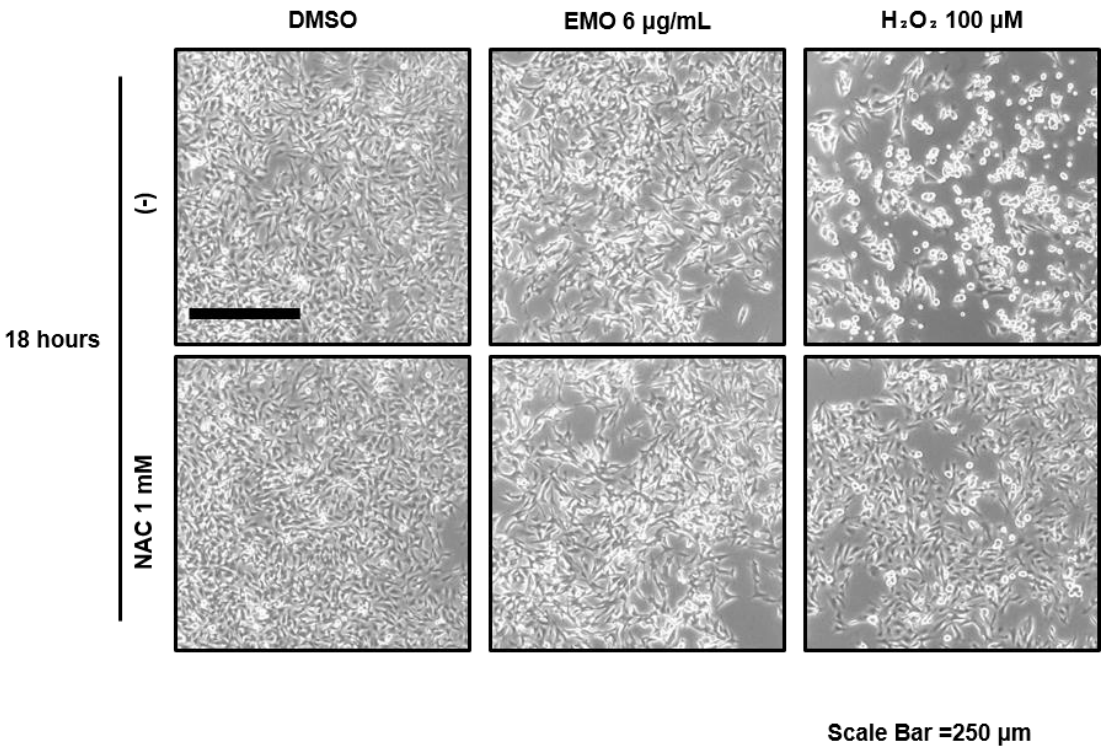

Figure S10 – The antioxidant N-acetyl-L-cysteine (NAC) does not eliminate the anti-proliferative effect of emodin. Scale bar, 250 µm.